1/27

4

The North Fiji Basin
Geology, Structure, and Geodynamic Evolution

Jean-Marie Auzende, Bernard Pelletier, and Jean-Philippe Eissen

ABSTRACT

As the result of intensive studies conducted by U.S., French, and Japanese scientific teams, the North Fiji Basin ridge, poorly known 10 years ago, is one of the most exhaustively investigated ridge axes of the world's oceans. Today, a ridge segment more than 800 km long and 100 km wide has been fully mapped with the Sea Beam and Furono echo sounders. This ridge axis shows four main segments characterized by the same morphostructural aspect and limits that characterize mid-oceanic ridges. Along the whole length of the axis, a water-column sample has been taken every 20 km and rock samples every 10 km. Different types of hydrothermal activity have been discovered and explored either during the *Nautile* cruise in 1989 or during the *Shinkai 6500* cruise in 1992. The most famous site is the "White Lady," located around 17°S; it is characterized by 285°C shimmering hot water, which is very poor in metallic elements, expelled through an anhydrite chimney. This water probably represents the low salinity end-member resulting from phase separation in the deep levels of the oceanic crust. Other active sites have been observed all along the axis showing different characteristics such as low-temperature diffusion zones. Even though some parts of the North Fiji Basin remain poorly investigated, the newly acquired data from the ridge axis and from the eastern and northwestern parts allow us to develop a new tectonic model of basin evolution since its creation 12 m.y. ago.

1. INTRODUCTION

The study of the North Fiji Basin (NFB) (Fig. 4.1) started between 20 and 25 years ago with focused efforts on selected areas and large scale profiling across the basin mainly conducted during U.S. cruises (Scripps Institution of Oceanography, Hawaii Institute of

Jean-Marie Auzende • IFREMER/CB, 29280 Plouzané, France. *Present address*: ORSTOM, BPA5, Nouméa, New Caledonia. *Bernard Pelletier* • ORSTOM, Nouméa, New Caledonia. *Jean-Phillippe Eissen* • Antenne ORSTOM-IFREMER/CB, 29280 Plouzané, France.

Backarc Basins: Tectonics and Magmatism, edited by Brian Taylor, Plenum Press, New York, 1995.

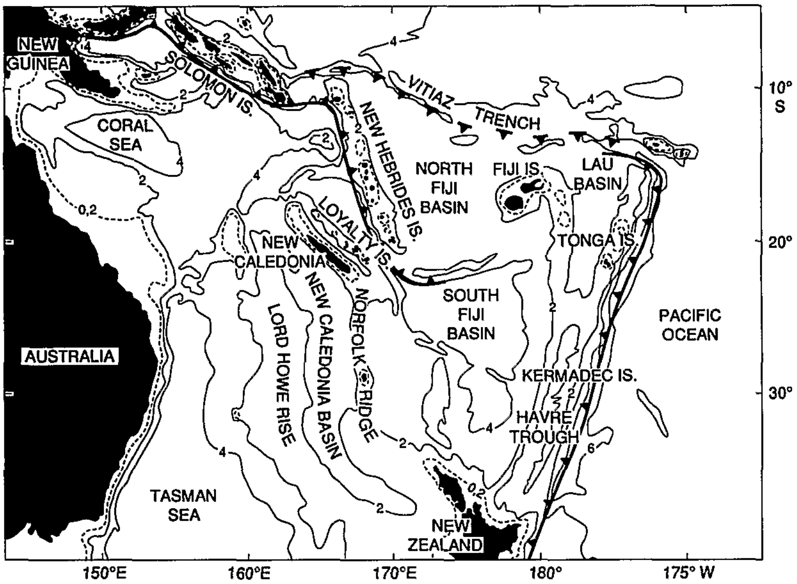

FIGURE 4.1. General geodynamic setting of the North Fiji Basin (NFB) in the SW Pacific.

Geophysics, and Woods Hole Oceanographic Institution) and French ORSTOM cruises. Since 1976, ORSTOM (Institut Français de Recherche Scientifique pour le Développement en Coopération) has conducted the EVA (Evolution des Arcs insulaires) program, which has been partly devoted to the study of the Lau and North Fiji basins. Fifteen cruises have been conducted in different areas, especially in the New Hebrides arc domain, in the southernmost part of the basin around the Matthew–Hunter zone, and more recently in the northwestern part of the basin.

The SEAPSO (Sea Beam Pacifique Sud Ouest) program in 1985 represented the first coordinated approach by French teams for backarc basin studies. As a part of this program, IFREMER (Institut Français de Recherche pour l'Exploitation de la Mer), ORSTOM, and INSU (Institut National des Sciences de l'Univers) jointly explored the NFB where the existence of an axial ridge was assumed but not demonstrated. One of the major results of the SEAPSO-Leg 3 cruise of the R.V. *Jean Charcot* was the partial mapping of an active accreting ridge in this marginal basin.

On the basis of the SEAPSO cruise results, Japanese and French scientists decided to undertake a joint project to study the rift systems of the western Pacific. This project, STARMER, coordinated by IFREMER in France and the Science and Technology Agency (STA) in Japan, was initiated in 1987. Its objective was a five-year interdisciplinary (geology, geochemistry, and geophysics) study of the NFB ridge. Since this date, seven cruises have been conducted, representing more than nine months at sea. Four cruises were dedicated to surface-ship surveys, including swath bathymetric mapping, geophysical profiling, water sampling, gravity coring, and dredging. The three others were diving cruises using the *Nautile* (June–July 1989), the new Japanese submersible *Shinkai 6500* (September–November 1991), and *Cyana* (December–January 1992).

Simultaneously, U.S., German, and SOPAC (South Pacific Applied Geoscience Commission) teams conducted SeaMARC, Sea Beam, and GLORIA (geologic long range inclined asdic) surveys on selected areas, especially in the northern and northeastern parts of the NFB. In total, more than 20 months of ship time have been spent in the basin in the past 10 years. The result of these efforts is an extensive multibeam bathymetric coverage of the central spreading axis, detailed rock and water sampling along the axis, and *in situ* observations by deep-tows and submersibles.

The NFB is one of the marginal basins located at the converging boundary between the Pacific and Australian major plates (Fig. 4.1). It lies between the New Hebrides arc to the west, the Fiji Platform to the east, the Vitiaz fossil subduction zone to the north, and the arcuate Matthew–Hunter zone to the south. Different models for opening of the NFB have been proposed (Chase, 1971; Gill and Gorton, 1973; Falvey, 1975; Dubois *et al.*, 1977; Malahoff *et al.*, 1982a; Auzende *et al.*, 1988b). These authors suggest that the opening of the basin started 10 m.y. ago after the locking of the Vitiaz subduction by the Ontong–Java Plateau and the reversal of its subduction polarity. This change of polarity involved the clockwise rotation of the New Hebrides arc and by secondary effect the anticlockwise rotation of the Fiji Platform. This first phase implies a NW-SE-trending spreading axis and N45° to N55° flowlines for the opening motion. The second phase resulted in the beginning of the collision of the New Hebrides arc with the d'Entrecasteaux and Loyalty Islands ridges (Daniel, 1982; Louat, 1982; Monzier *et al.*, 1984,1990), the change of the traction stresses to an E-W direction, and the emplacement of the N-S-trending spreading center in the central part of the basin. During this time N-S spreading occurred in the northern part of the basin and north of the Fiji Islands (Auzende *et al.*, 1988a,b).

1.1. Bathymetry and Structure

Bathymetric data concerning the NFB were rare before the SEAPSO III cruise of the R.V. *Jean Charcot* (December 1985) and the five surface cruises of the STARMER project. The only existing data were general and imprecise maps (Chase, 1971; Mammerickx *et al.*, 1971) or more detailed local surveys (Halunen, 1979; Kroenke *et al.*, 1987, 1991). The NFB was then called the North Fiji Plateau, and the main feature mapped was a 3000-m-deep flat area occupying the whole central part of the basin.

The bathymetric map shown in Fig. 4.2 (Mazé *et al.*, 1992, unpublished map) results from the compilation of all the available bathymetric data; it combines good-quality classical bathymetric surveys and recent multibeam surveys performed mainly within the SEAPSO and STARMER projects. This map especially uses the data from the maps of Monzier *et al.* (1984, 1991), Auzende *et al.* (1990b, 1992b) and Urabe *et al.* (1992). It shows the different physiographic zones characterizing the NFB. We have divided the basin into five physiographic and structural provinces: the western basin, the central spreading ridge, the eastern basin, the northwestern basin, and the northeastern basin.

1.1.1. The Western Basin

This domain is located south of the Hazel Holme Ridge (14°S) between the New Hebrides arc and 173°E (Fig. 4.2). It is still poorly known and contains the largest portion of old crust of the basin, including the initial NW-SE spreading center (Auzende *et al.*, 1988b; Pelletier *et al.*, 1993a). Although some topographic features exist, especially in its southern

FIGURE 4.2. Bathymetric map of the NFB. This map results from a compilation (J.P. Mazé) of all multibeam data existing on the NFB (SEAPSO, Proligo, STARMER, Multipso cruises). The contour interval is 200 m. CSR: central spreading ridge; WB: western basin; E: eastern basin; NWB: northwestern basin; NEB: northeastern basin. Locations of Figs. 4.3, 4.5, 4.7, and 4.11 are shown.

part (south of 17°S), the western basin is mainly characterized by gently undulating and flat areas 3200–3300 m deep. The primitive oceanic crust topography is smoothed or obliterated by sedimentary cover which thickens toward the west from 0.1 s to more than 0.5 s of two-way travel time (Luyendyck *et al.*, 1974; Halunen, 1979; Kroenke *et al.*, 1994). The thickest sediments occur in the westernmost part of the basin along the New Hebrides arc, especially east of the central New Hebrides islands where the thickness reaches 1-s two-way travel time in seismic reflection profiles (Luyendyck *et al.*, 1974; Pelletier *et al.*, 1988).

From 17°20′S to 20°50′S, the westernmost part of the western basin is characterized by the N150° trending southern New Hebrides backarc troughs (Fig. 4.2) (Monzier *et al.*, 1984, 1991; Récy *et al.*, 1990; Price *et al.*, 1993). These troughs deepen southward from 2800 to 3600 m and are flanked eastward by a N150° volcanic ridge with an average depth of 1000 m and rising to 650 m above sea level at Futuna Island. A secondary N150°–170° trending volcanic ridge (600 to 1800 m deep) lies 30 km east of the Futuna Ridge. Isolated volcanoes exist farther east; one of them, the Constantine Bank, shoals to a depth of 104 m (Monzier *et al.*, 1984).

The morphology of the southern part of the western basin is still largely unknown but appears to be complex and characterized by NE-SW-trending structural features (Fig. 4.2)

(Monzier *et al.*, 1984,1991). Around 21°S, 172°E, two N40–45° trending ridges rising to a depth of 2000–2200 m and enclosing a 3600-m depression are the most prominent features and likely a major tectonic element of this southern area. Because NW-SE trending magnetic anomaly lineations exist immediately to the southeast, this paired trough-ridge is interpreted as a fracture zone.

Other important tectonic features are located at 17°30′S, 172°E in the central eastern part of the western basin, where NE-SW-trending, steep-sided, linear ridges rise to 1300 m and are commonly interrupted by 3000–3300-m depressions (Halunen, 1979). The ridge area, also characterized by absence of sediments, high heat flow, and presence of shallow earthquakes, has been interpreted as an active NE-SW spreading center (Halunen, 1979).

1.1.2. The Central Spreading Ridge

Locally recognized from bathymetric and magnetic profiles (Chase, 1971; Malahoff *et al.*, 1982a; Maillet *et al.*, 1986), the central spreading ridge (CSR) was for the first time partially multibeam-mapped during the SEAPSO III cruise of the R.V. *Jean Charcot* (December 1985) (Auzende *et al.*, 1986a,b, 1988a). Up to now within the French–Japanese joint STARMER project it has been mapped between 14°30′S and 21°40′S on more than 1° width by multibeam bathymetric full coverage (Auzende *et al.*, 1990b; Urabe *et al.*, 1992; Fig. 4.3). The ridge axis can be divided into four major segments, with lengths varying from 120 to more than 200 km, that are described below from south to north.

1.1.2.1. The Southernmost Segment. The southernmost segment is about 120 km long between 21°40′S and 20°30′S. It is characterized by a N-S trend and a complicated morphology of alternating ridges reaching 2500-m depth and depressions reaching below 3000 m. The atypical morphology and the lack of *in situ* observation make it difficult to locate precisely the present-day spreading axis on this segment. Only magnetic lineation analysis (Maillet *et al.*, 1989; Ruellan *et al.*, 1989) confirms the existence of an active spreading axis centered on 174°05′E. The transverse bathymetric profile of Fig. 4.4 illustrates this atypical morphology intermediate between fast and slow spreading ridges (Macdonald, 1983; Karson *et al.*, 1987).

1.1.2.2. The 310-km-Long North-South Segment. The 310-km-long north-south segment, between 21°S and 18°10′S, is apparently the simplest segment. Its linear ridge axis crosses a 2800-m-deep flat-topped dome cut in its center by a graben that is a few hundred meters wide and a few tens of meters deep. The width of the axial ridge, limited by the 3000-m isobath, is about 20 km. On both sides, the dome is flanked by symmetrical grabens more than 3000 m deep and trending N-S. The southern and northern tips of this segment exhibit V-shaped features interpreted as inner and outer pseudofaults of propagating rifts (de Alteris *et al.*, 1993; Ruellan *et al.*, 1994). In the middle part of the segment, around 19–19°40′S, symmetrical oblique volcanic lines crosscut the N-S oceanic structural grain. On the northwestern side of the area west of the inner pseudofault, the oceanic bottom shows successive arcuate ridges abutting the pseudofault. These peculiar features can be either interpreted as fossil overlapping spreading centers (OSC) (Ruellan *et al.*, 1994) or as failed rifts of a propagating rift system (de Alteris *et al.*, 1993).

1.1.2.3. The N15° Segment. The N15° segment is about 120 km long and shows spectacular along-strike morphological variation. In its southern part from 18°10′S to 17°55′S,

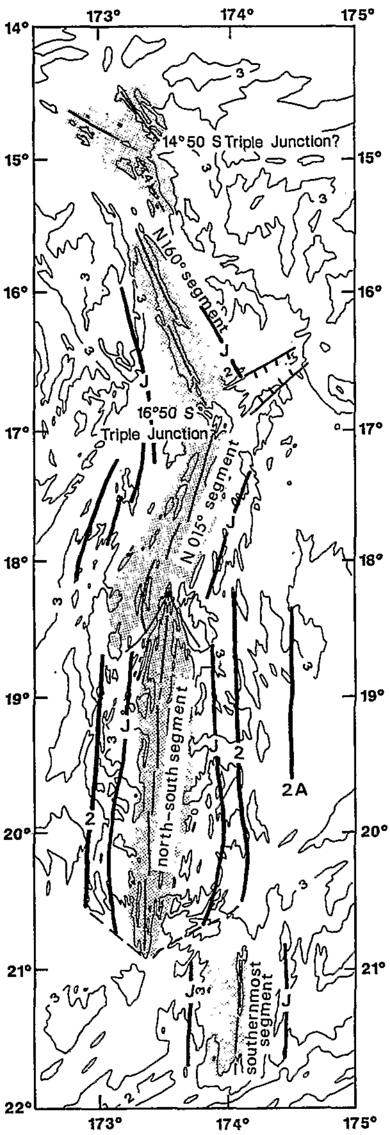

FIGURE 4.3. Simplified bathymetry (contour interval = 1000 m) and magnetic lineations (heavy lines) along the central spreading ridge from Auzende *et al.* (1990c) and de Alteris *et al.* (1993) (after Auzende *et al.*, 1994b). The present-day axis is shown with medium lines. In gray: anomaly 1; J: Jaramillo anomaly (1 Ma); 2: anomaly 2 (1.98 Ma); 2A: anomaly 2A (2.6–3.5 Ma). The ages of anomalies are after Cande and Kent (1992).

the present-day axis is not well defined and the accretion is distributed over numerous small volcanoes scattered over a wide area. This zone corresponds to the change of direction of the central spreading ridge from N-S to N15°. North of 17°55′S, the spreading axis is represented by a double ridge less than 2500 m high bounding a 2–3-km-wide, 200–300-m-deep graben. At the northern tip of the N15° segment, close to the 16°50′S triple junction, the ridge axis is located on the top of a shallow massif culminating at less than 1900 m deep and cut by a graben 500 m to 2 km wide and 200 m deep. This area is the site of the active hydrothermal vents explored by *Nautile* and *Shinkai 6500* (see following). The N15° axial ridge is flanked by curved grabens more than 3000 m deep interpreted by Ruellan *et al.* (1994) as fossil OSCs.

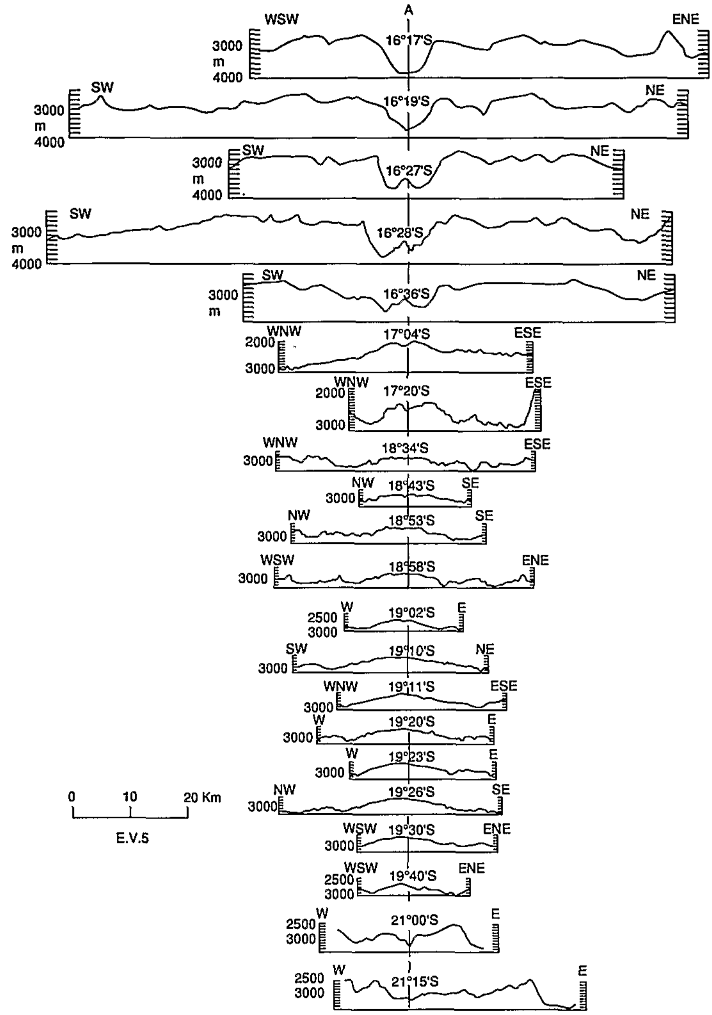

FIGURE 4.4. Transverse bathymetric profiles across the different segments of the central spreading ridge (16°17′S to 21°15′S). A: ridge axis.

1.1.2.4. The N160° Segment. The N160° segment is about 200 km long and can be described as three parts (Auzende *et al.*, 1991a, 1994a; Gracia-Mont, 1991, 1992; Jarvis *et al.*, 1993; Figs. 4.5 and 4.6): (1) *From 16°50S to 15°30S* the spreading axis is located in a 4000–4500-m-deep graben located between two subvertical walls. The average width of the graben is 8 km along the whole segment. In its axial part, the graben is cut by a 2–3-km-wide, 400–500-m-high ridge (Fig. 4.4). This morphology is very similar to those described at slow spreading (less than 40 mm/yr) ridges like the Mid-Atlantic Ridge (Kappel and Ryan, 1986; Karson *et al.*, 1987; Karson, 1990; Gente *et al.*, 1991). Around 16°10S, the remarkable linearity of the N160° axis is interrupted by a slight curve toward the north, offsetting the graben by about 4 km. On both sides the active domain is flanked by a large volcanic massif that shallows to less than 1700 m deep. The width of the volcanic massif

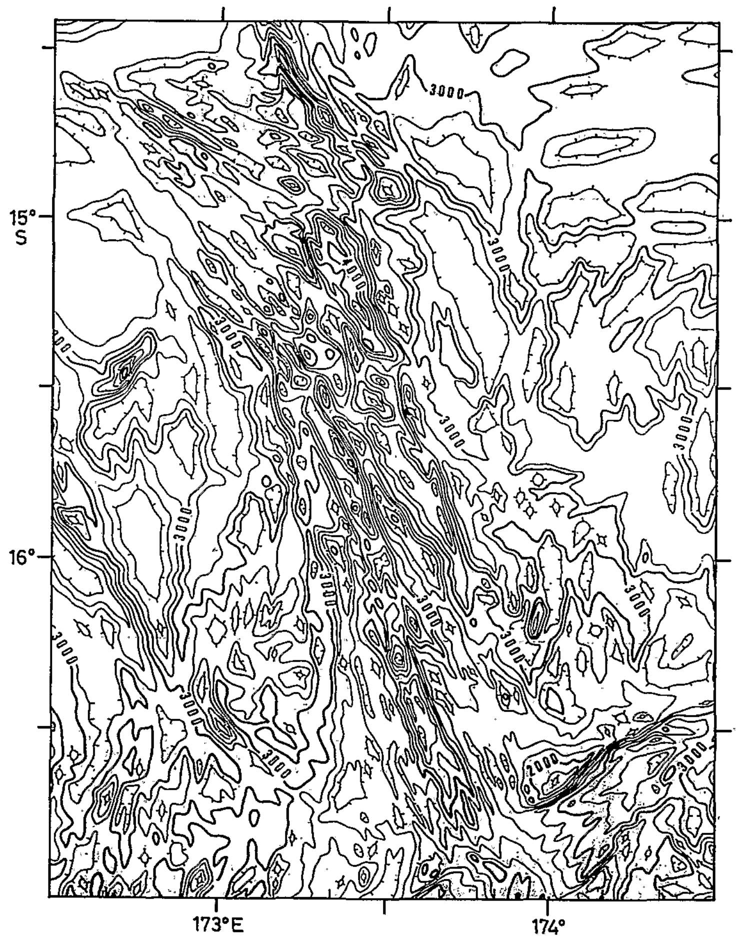

FIGURE 4.5. Bathymetry of the N160 segment and of the 14°50′S triple junction (enlargement of Fig. 4.2). The contour interval is 200 m.

decreases from 100 km in the south to a few kilometers in the north until it disappears north of 15°30′S. The magnetic data analysis allows an estimate of the beginning of the volcanic construction and the massif uplift at about 1 Ma. This uplift affects an older oceanic crust as demonstrated by the age of the sediments sampled from the northern edge of the N55° trending graben located east of the 16°50′S triple junction (Lagabrielle *et al.*, 1994). (2) *Between 15°30′S and 15°00′S* the accretion is distributed over a wide domain of two 60-km-long, 4000-m-deep en echelon grabens offsetting the axis by about 40 km to the northeast. Each of these grabens is made up of a succession of 10-km-long en echelon segments (Fig. 4.6). In this area, the magmatic supply appears to be concentrated along a narrow ridge that separates the grabens. For the past 1 m.y. the accretion seems to have been mainly amagmatic (Gracia-Mont, 1991, 1992). (3) *North of 15°00S* the spreading axis becomes more complex and is located within two distinct branches. The western one, trending N120°, is characterized by a 4-km-wide, 4000-m-deep graben that crosscuts an older oceanic crust showing different trends from N160° to N120°. The northern branch consists

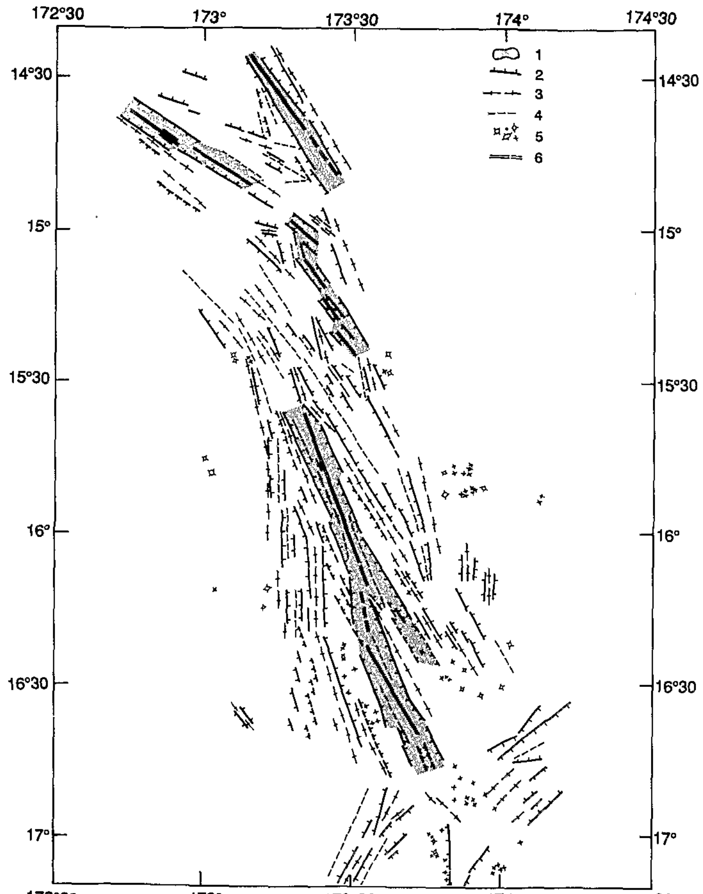

FIGURE 4.6. Structural map of the N160 segment and of the 14°50′S triple junction (after Auzende *et al.*, 1994a). 1: axial domain deduced from bathymetry and magnetic anomaly, 2: normal fault and scarps, 3: crests, 4: depressions, 5: isolated volcanoes, 6: ridge axis.

of a 2400-m-deep, N140°-trending ridge that connects with the N160° graben system at a 4000-m-deep depression at 14°50′S. This depression can be interpreted as a triple junction between the N160° and N120° grabens and the N140° ridge (Auzende *et al.*, 1994a).

1.1.3. The Eastern Basin

The eastern basin occupies the area between the Fiji Islands and the central spreading ridge. On the basis of different arguments, a spreading ridge was postulated west of Fiji (Sclater and Menard, 1967; Chase, 1971; Brocher and Holmes, 1985). Few recent data exist for this area, except a full-coverage, one-square-degree bathymetric survey located immediately west of Fiji (Fig. 4.7). This area is underlain by important shallow seismicity with strike-slip (Hamburger and Isacks, 1988, 1994) and normal-fault-type focal mechanism solutions (Louat and Pelletier 1989; Pelletier and Louat, 1989). Previously interpreted as a strike-slip deformation zone (Auzende *et al.*, 1986b), this area was recently reinterpreted in

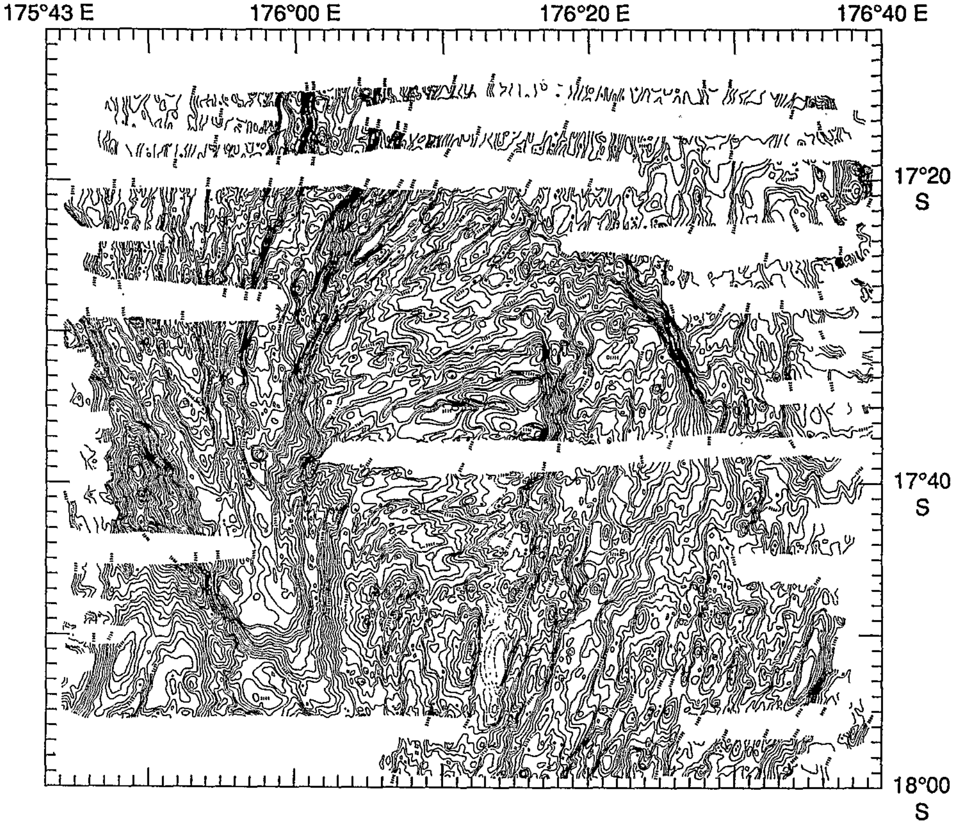

FIGURE 4.7. Sea Beam bathymetry of the West Fiji area (after Auzende *et al.*, 1988a). The contour interval is 50 m.

terms of a propagating rift (Auzende *et al.*, 1993, 1994b). The main morphostructural units of the area are represented in Fig. 4.8.

1.1.3.1. The Propagating Ridge (PR) and Its Tip (PT). The PR is located in the western part and comprises a central ridge bounded by two grabens. The eastern graben is well developed with a constant width of 10 km and depth of 4000 m. The western graben is narrower (2–3 km) and shallower (3000 m). The central ridge is 7 to 8 km wide and 2750 m deep. Its N-S to N05° trend changes to N155° at its southern tip. The width of the PR varies from 40 km in the north to 8 km in the south. South of 17°44′S, the ridge disappears and is replaced by a 3000 m deep flat area limited by converging faults. This flat area is similar to the "propagating tip" described by Hey *et al.* (1986) in the case of the 95.5°W propagating rift on the East Pacific Rise close to the Galapagos.

1.1.3.2. The Pseudofaults. The outer pseudofault (OPF) corresponds to a N155°-trending fault bounding the propagating system on the west. This fault separates the propagating from the "normal" oceanic bottom grain trending N15–20°. The inner pseudofault (IPF) is repeated north of 17°35′S (Fig. 4.8, dashed line, top center), with a N15° fault

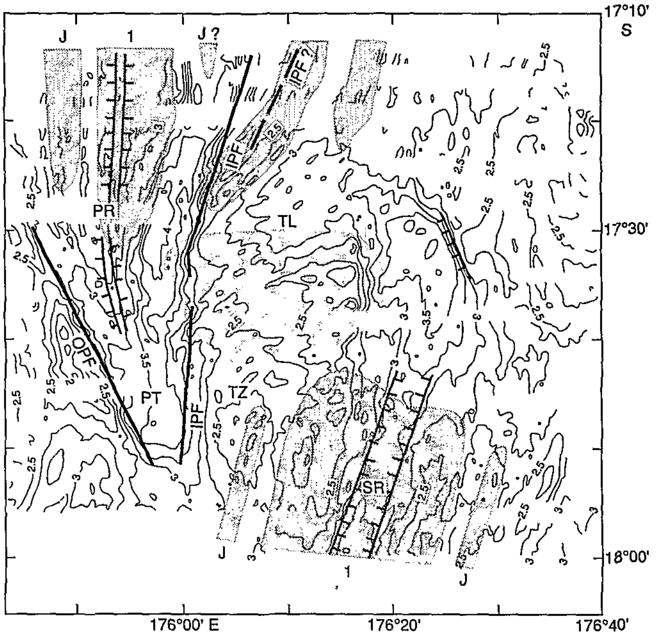

FIGURE 4.8. Structural sketch of the West Fiji Ridge (after Auzende *et al.*, 1993). PR axis: propagating axis; PT: propagating tip; OPF: outer pseudofault; IPF: inner pseudofault; SR: southern rift; TL: transferred lithosphere; TZ: transform zone. Main positive and negative magnetic anomaly lineations are underlined in gray and light gray respectively. Anomalies 1 and J are labeled.

converging toward the OPF with a 40° angle to the west and a more diffuse lineament trending N30° and converging with the OPF with a 55° angle to the east. South of 17°35′S, there is a unique fault converging with the OPF at a 20° angle.

1.1.3.3. The Southern Ridge (SR). This SR is located in the southeastern part of our survey (Fig. 4.8) and is characterized by a 3000-m-deep, few-kilometer-wide axial graben trending N10°. In the eastern part of the domain, the failed rift is represented by a succession of N10–N15° trending ridges abutting a N150° fault. These ridges are 2 to 3 km wide and 2750 m deep. They probably represent the old spreading axis abandoned during the southward propagation of the western active rift.

1.1.3.4. The Transform Zone (TZ) and the Transferred Lithosphere (TL). The junction between the propagating rift and the southern ridge is a wide zone of arcuate small ridges representing a transform zone as defined by Hey *et al.* (1986) on the East Pacific Rise. The TL is located north of the TZ and comprises fan-shaped structures deepening to 3000 m in the northern part.

The close structural similarities between this area and the Galapagos propagating rift confirm the interpretation of an active spreading axis. The spreading rate was estimated to be 30 mm/yr by Louat and Pelletier (1989) from seismicity analysis and kinematic reconstruction of the Lau and North Fiji basins. The width of the propagating rift area is consistent with this rate estimate (see following).

1.1.4. The Northwestern Basin

The northwestern basin, located north of 14°S and west of 174°E between the northern part of the New Hebrides island arc to the west and the Vitiaz Trench to the east, has been the subject of different speculations and interpretations, caused mainly by the lack of data. It was interpreted as (1) the result of a late Miocene fan-shaped opening along a median NW-SE-trending axis (Falvey, 1975; Malahoff *et al.*, 1982a; Auzende *et al.*, 1988b), (2) an old piece of Pacific plate (Chase, 1971; Luyendyck *et al.*, 1974), or (3) Australian plate (Halunen, 1979) trapped behind the Vitiaz paleotrench. Recently, the bathymetry and main morphostructural units of the whole northwestern part of the NFB have been recognized during the EVA 14 (1987) and Santa Cruz (1991) cruises of R.V. *Coriolis* and *Le Noroît*, respectively, and are described here (Pelletier *et al.*, 1988, 1993a,b) (Figs. 4.9 and 4.10).

1.1.4.1. The N-S-Trending Northern New Hebrides Backarc Troughs. The N-S-trending northern New Hebrides backarc troughs were previously known south of 12°S (Charvis and

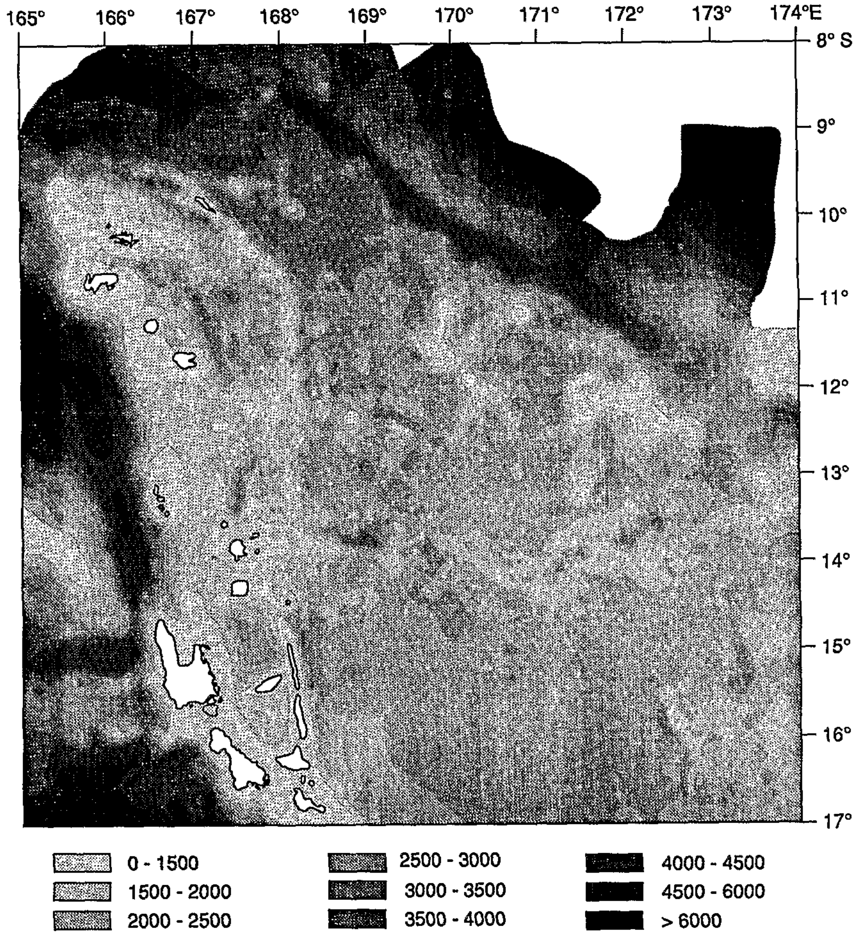

FIGURE 4.9. Bathymetric map of the northwestern basin.

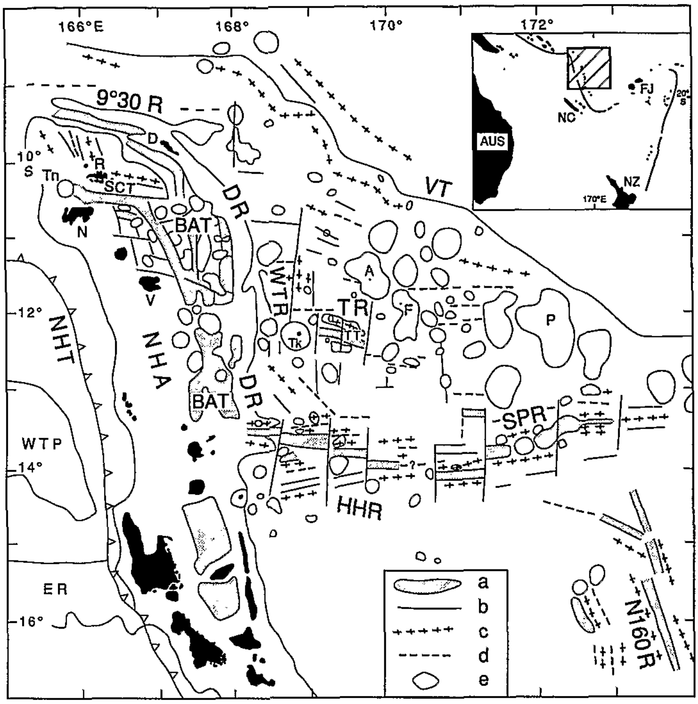

FIGURE 4.10. Structural map of the northwestern basin (after Pelletier *et al.*, 1993a). The studied area is shown in insert. AUS: Australia; NC: New Caledonia; FJ: Fiji; NZ: New Zealand. NHT: New Hebrides Trench; NHA: New Hebrides arc; VT: Vitiaz Trench; BAT: backarc troughs domain; 9°30 R: 9°30′S Ridge; DR: Duff Ridge; WTR: West Tikopia Ridge; TR: Tikopia Ridge; HHR: Hazel Holme Ridge; SPR: South Pandora Ridge; N160 R: N160 ridge of the central spreading ridge; TT: Tikopia Trough; SCT: Santa Cruz Trough; WTP: West Torres Plateau; ER: d'Entrecasteaux ridge. Islands and reefs are in black. D: Duff Islands; R: Reef Islands; Tn: Tinakula Island; N: Ndende Island; V: Vanikoro Island; Tk: Tikopia Island; A: Anuta Island; F: Fatutaka Island; P: Pandora Bank. (a) trough and depression; (b) structural trend and fracture; (c) structural high; (d) structural low; (e) volcanic high.

Pelletier, 1989; Récy *et al.*, 1990; Johnson *et al.*, 1993) and extend from 13°30′S to 9°30′S, east of the New Hebrides arc platform in the westernmost part of the basin. The troughs are formed by volcanic cones and ridges bounding N-S trending, 3000–3500-m-deep depressions, between a N-S- to NNW-SSE-trending major scarp to the west and Duff ridge to the east. They are filled by large volcanic highs at 12°S and 10°30′S and are 60 km wide south of 12°S and widen northward up to 100 km at 10°45′S. At 10°30′S the western part of the troughs abuts the N95° trending Santa Cruz trough, which cuts the arc platform.

1.1.4.2. The Duff Ridge. The Duff Ridge separates the backarc troughs from the central part of the northwestern basin. It is a continuous volcanic ridge more than 400 km long and 30 km wide, which strikes N-S and rises to around 1500 m south of 10°45′S. It trends NW-SE and shoals to 20 m farther north. The volcanic Duff Islands are located in the northernmost tip of the ridge. Duff Ridge is interpreted as a fossil volcanic line related to the New Hebrides subduction.

1.1.4.3. The Tikopia, West Tikopia, and 9°30′S Ridges. The Tikopia, West Tikopia, and 9°30′S ridges are a succession of orthogonal ridges, interpreted as spreading ridges or transform zones, lying in the axial part of the northwestern basin, which generally deepens to the north from 3200 to 4200 m. Tikopia ridge trends E-W and is located around 12°30′S between the Tikopia volcano and island at 168°45′E and the volcanoes located south of Fatutaka Island at 170°45′E. East of the large Tikopia volcano (3500 m high, 35 km wide at its base), the ridge is a 50-km-wide, N90°–100° trending elongated dome cut along strike by a 10-km-wide, 65-km-long trough (4200 m deep) bounded by 1000–1500-m-high scarps. Fresh basalts have been dredged on the northern wall of the trough. West Tikopia Ridge is a N-S-trending, discontinuous ridge composed of aligned seamounts rising to 800 m west of the Tikopia volcano along 168°30′E from 12°20′S to 10°45′S. The 9°30 ridge is an almost continuous, N100° trending volcanic ridge from 165°45′E to 168°15′E north of the New Hebrides arc platform and the Duff Islands. The 9°30 ridge ends to the east at a large volcanic massif shoaling to 10 m in the northern prolongation of the West Tikopia Ridge.

Numerous volcanic highs, including *Anuta and Fatutaka Islands and Pandora Bank,* are located in the eastern part of the area between 10°30′S to 13°S and 169°E to 174°E , south of the Vitiaz paleotrench. These volcanic highs, previously considered as a part of the inactive Vitiaz arc, do not constitute a continuous chain but are isolated and occur as far as 240 km from the Vitiaz paleotrench. They constitute a series of massifs aligned on N-S lineaments. No volcanic arc lies immediately south of the Vitiaz paleotrench. However, a narrow ridge rising to about 2000 m between 12° and 11°S and a narrow and discontinuous swell (3200–3400 m deep) north of 10°30′S parallel the Vitiaz Trench (4500–6000 m deep), which shows a succession of NW-SE and E-W trending troughs.

The northwestern basin is separated from the rest of the basin by a complex series of E-W-trending ridges and troughs called the Hazel Holme fracture zone by Chase (1971). Right-lateral or left-lateral strike slip or even compressional motions have been proposed along this enigmatic feature (Luyendyck *et al.*, 1974; Halunen, 1979; Eguchi, 1984; Hamburger and Isacks, 1988,1994), which can be described as two parts.

1.1.4.4. The Hazel Holme Ridge, which corresponds to the western part of the Hazel Holme fracture zone of Chase (west of 171°E), was partly surveyed during the EVA 14 and Santa Cruz cruises and interpreted as an active extensional zone (Pelletier *et al.*, 1988, 1993a; Charvis and Pelletier, 1989; Louat and Pelletier, 1989). This seismically active feature is composed of several parallel narrow ridges and deep troughs trending N80–100° and extending over a maximum width of 120 km. The troughs are, on average, 3500–4000 m deep and are bounded by 500–1000-m-high scarps. The deepest trough (4500 m deep at about 169°E) is located in the axial part of the feature and appears to be right-laterally offset. West of 168°30′E the width of the ridge decreases, lateral troughs disappear, and a 2500–3500-m-deep E-W trough is bounded by symmetrical ridges rising to 1700 m. This trough ends at 168°10′E where it connects with the southern tip of the northern New Hebrides backarc troughs. The bathymetric profiles across the area exhibit a slow spreading ridge morphology.

1.1.4.5. The South Pandora Ridge, which corresponds to the eastern part of the Hazel Holme fracture zone of Chase (1971), was explored between 171°E and 173°30′E during a R.V. *Kana Keoki* reconnaissance cruise (1982) and near 174°E by a SeaMARC survey during the R.V. *Moana Wave* cruise (1987); it is interpreted as an E-W trending active slow spreading ridge within a broad transform domain (Kroenke *et al.*, 1991; Price and Kroenke, 1991). The ridge is 110 km wide and is cut by numerous transform offsets. It is composed of a series of E-W trending segments cut along strike by a central trough that is 10 to 20 km wide and 500 to 4500 m deep. The axial trough is flanked by 1000–2000-m-high scarps and is locally filled by large volcanoes rising in some places to sea level. Fresh pillow basalts recovered on the South Pandora Ridge have geochemical characteristics intermediate between mid-ocean ridge basalts (MORBs) and ocean island basalts (OIBs) (Price *et al.*, 1990; Price and Kroenke, 1991; Sinton *et al.*, 1994).

1.1.5. The Northeastern Basin

The northeastern basin is located east of 174°E and west of the northern Lau Basin (Fig. 4.2), between the Fiji Platform and the North Fiji fracture zone in the south and an imprecisely located lineament in the north that separates the young NFB oceanic crust from the old Pacific crust. This lineament is marked by a succession of deep troughs (Alexa Trough, Rotuma Trough, Horn Trough; Brocher, 1985) and connects the Vitiaz Trough to the west and the northern tip of the Tonga Trench to the east. Although some restricted areas have been recognized (see below), the overall structure of the northeastern basin is largely unknown. The northeastern basin is now the least-known part of the NFB.

On the basis of an aeromagnetic survey over the entire area, Cherkis (1980) reported E-W-trending magnetic lineations and proposed an active spreading center located near 14°30′S from 175° to 178°E and near 14°S from 178°E to 180°. The only area explored by surface ship is located north of Viti Levu Island between 176°30′E and 178°E and 13°30′S and 15°S (Halunen, 1979; Brocher, 1985). Halunen (1979) described a prominent NW-SE trending paired ridge-trough in the northwest part, more subdued WSW-ENE trending topography in the southwest, and uniform sediment cover about 0.08 s double-travel-time thick. On the basis of WNW-ESE magnetic lineations and bathymetric trends offset by an oblique NNW-SSE trough at 177°30′E and interpreted as a pseudofault, Brocher (1985) proposed a WNW-ESE inactive spreading center at 14°30′S and 14°S located respectively west and east of a fossil propagating rift at 177°30′E.

More recently, a multibeam bathymetric survey of a N-S elongated area at 177°–177°30′E from 13°50′S to 16°40′S was conducted during the R.V. *Sonne* cruise SO-35 (von Stackelberg *et al.*, 1985; von Stackelberg and von Rad, 1990). The different morphostructural units are described below from north to south (Fig. 4.11).

1. A 3500-m-deep, 10-km-wide steep-sided trough trends N120° at 14°05′S and is bounded by linear ridges rising to 2200 m. This trough, also described by Halunen (1979), corresponds to the northwestern extension of the pseudofaults of Brocher (1985) and is surprisingly interpreted by von Stackelberg and von Rad (1990) as a short narrow basin possibly belonging to the Vitiaz Trench lineament.

2. Two N120° trending narrow ridges, rising to 2400–2700 m and enclosing a 2900-m-deep depression, are observed at 14°30′S and are interpreted, following Brocher (1985), as an extinct spreading center. Although magnetic lineations are associated with these ridges, the unidentified anomalies do not allow an estimate of the age for the spreading. Altered ferrobasalts derived from a parental MORB magma and covered with hydrothermal Mn crusts were recovered from these ridges (Sinton *et al.*, 1985; Johnson and Sinton, 1990).

3. Volcanoes are present between 14°50′S and 15°15′S.

4. Two N70° trending prominent and parallel ridges exist at 15°40′S and 15°50′S. The northern one, called the Braemar Ridge, rises to 1600–1900 m deep and is bounded to the north by a 3600-m-deep depression. The southern ridge is 2000–2200 m deep and is

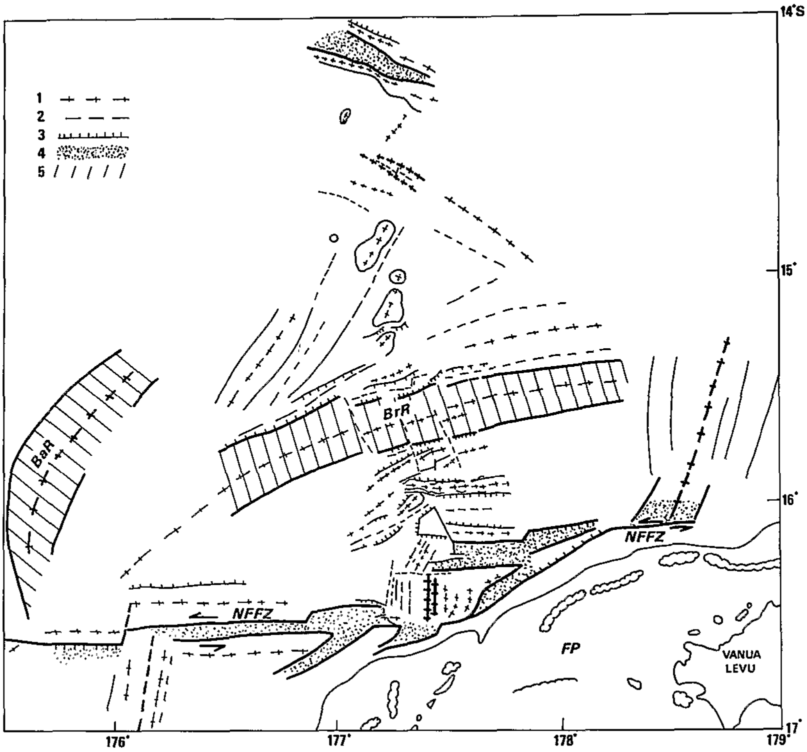

FIGURE 4.11. Structural sketch of a part of the northeastern basin based partly on the bathymetric map obtained during the R.V. *Sonne* cruise SO-35 (von Stackelberg *et al.*, 1985; von Stackelberg and von Rad, 1990), the GLORIA image (Jarvis *et al.*, 1994) and the map of Fig. 4.2. 1: structural high; 2: structural low; 3: scarp; 4: main trough; 5: main ridge. FP: Fiji Platform; NFFZ: north Fiji fracture zone; BrR: Braemar Ridge; BaR: Balmoral Ridge.

narrower than and separated from the Braemar Ridge by a 2900-m-deep depression. These two ridges are interpreted as uplifted faulted blocks of Pliocene volcanics and volcaniclastics derived from the fossil Fiji volcanic arc and deposited in a forearc basin between the Vanuatu–Fiji–Lau–Tonga arc and the Vitiaz Trench lineament (von Stackelberg and von Rad, 1990).

5. An E-W trending ridge lies at 15°55′S and appears to be made up of aligned volcanoes.

6. A 30–40-km-wide pull-apart basin with N-S structural trends, centered at 177°25′E between 16°10′S and 16°35′S, is developed between an E-W trending 2000-m-deep ridge and 3400–4000-m-deep troughs (von Stackelberg and von Rad, 1990). Fresh MORB and backarc basin basalts (BABB) lavas with hydrothermal sulfide mineralization have been recovered in the pull-part basin.

The topography of the area immediately north of the Fiji Platform is controlled by the active left-lateral north Fiji fracture zone. The zone extends from the northern tip of the Tonga Trench to the central part of the NFB and marks the present-day boundary between the Pacific and Australian plates. The fracture zone is mainly composed of E-W structural trends with some pull-apart basins (Louat and Pelletier, 1989; Pelletier and Louat, 1989; Johnson and Sinton, 1990; Hughes Clarke *et al.*, 1993; Jarvis *et al.* 1994). The fracture zone has been partly imaged by SeaMARC (Kroenke *et al.*, 1991) and GLORIA during the SOPAC cruise in 1990 (Hughes Clarke *et al.*, 1993; Jarvis *et al.*, 1994). A second pull-apart basin trending N45° was found at 15°30′S, 178°40′E. The ridges located in the northeastern basin north of the Fiji Platform, like the Braemar Ridge and the Balmoral Ridge and Balmoral Reef farther west, are interpreted by Jarvis *et al.* (1994) to be pieces of the Fiji Platform rifted away by successive spreading segments (pull-apart basins) during changes in the location of the north Fiji fracture zone.

2. MAGNETISM AND PALEOMAGNETISM

The first published data concerning the magnetism (Sclater and Menard, 1967; Chase, 1971; Luyendyck *et al.*, 1974; Halunen, 1979) emphasized the complexity of the basin. These authors developed various interpretations of the magnetic lineations with different locations of spreading centers being proposed in the NFB south of the Hazel Holme Ridge. The area located to the north of the Hazel Holme Ridge was considered to be part of the old Pacific or Australian plates.

Paleomagnetic results from Vanuatu and Viti Levu indicate a clockwise rotation of the New Hebrides arc of about 28° since 6 Ma (Falvey, 1978) and a counterclockwise rotation of 21° since 4 Ma (James and Falvey, 1978) and of 90° since 7 Ma (Malahoff *et al.*, 1982b) of the Fiji Platform. These rotations and the polarity reversal from the Vitiaz to the New Hebrides subduction since 10–8 Ma are the basis for the hypothesis of a NW-SE trending spreading center northwest of Fiji and an E-W spreading axis north of Fiji (Falvey, 1978; Malahoff *et al.*, 1982a,b).

An aeromagnetic survey carried out by the National Oceanic and Atmospheric Administration (NOAA) and the U.S. Naval Research Project in 1979 (Cherkis, 1980; Larue *et al.*, 1982; Malahoff *et al.*, 1982a, 1994) defined magnetic lineations in the NFB which have been differently interpreted by different authors. After reprocessing these aeromagnetic data, Auzende *et al.* (1988b) proposed a new interpretation of the magnetic lineations. In the central basin a very clear N-S axial lineation is bounded by two parallel lineations identified as the J (Jaramillo) (1 Ma) and 2 (1.9 Ma) anomalies (Cande and Kent, 1992). On the eastern limb of the axis, a possible 2A (2.6–3.5 Ma) anomaly can be distinguished but is not continuously identified on the western limb. In the western basin the magnetic pattern is dominated by NW-SE lineations crosscut by transverse N45° trending features interpreted as transform faults. The NW-SE lineations represent the trends of the initial stage of opening of the NFB between 10 and 3 Ma (Auzende *et al.*, 1988b) or 12? to 7 Ma (Pelletier *et al.*, 1993a). The magnetic pattern of the eastern basin is less well defined and shows indistinctly NW-SE trends mixed with N-S directions which are particularly dominant immediately west of the Fiji Islands. The northern and northeastern parts of the NFB are mainly characterized on the aeromagnetic survey by roughly E-W trending lineations that have not been dated.

In the northwestern basin recent data acquired during the EVA 14 and Santa Cruz cruises permit precise definition of the magnetic pattern (Pelletier *et al.*, 1988, 1993a,b). The magnetic map (Fig. 4.12) mainly shows two trends of lineations. NW-SE trending lineations disrupted by NE-SW transform faults occur both in the northern edge of the area along

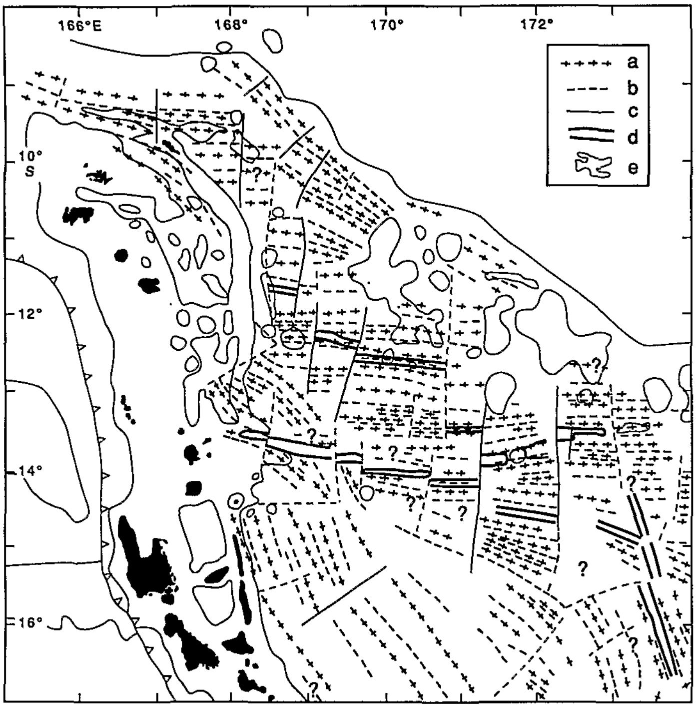

FIGURE 4.12. Map of magnetic anomaly lineations in the northwestern NFB (after Pelletier *et al.*, 1993b). (a) positive magnetic anomaly lineation; (b) negative magnetic anomaly lineation; (c) fault zone; (d) contour of the axial part of the spreading ridges; (e) contour of the main morphostructural features.

the Vitiaz Trench up to 8°30′S and in the southwestern part of the area along the New Hebrides arc, north and south of the western end of the Hazel Holme Ridge. Some NW-SE lineations are also present in the western side of the basin, north of 11°S from the eastern edge of the New Hebrides arc platform to the Duff Islands. The NW-SE lineations identified as anomalies 5A?–5 to 4 (12?–11 to 7 Ma) resulted from the initial opening of the basin in a NE-SW direction. E-W trending magnetic lineations disrupted by N-S transform faults are distributed over the entire central part of the northwestern basin from 9°S to 15°S and are flanked by the NW-SE lineations. The E-W trending lineations identified as anomalies 3A to 2A (7 to 2.5 Ma) resulted from a second stage of opening in a N-S direction and are associated with the South Pandora, Tikopia, and 9°30′S ridges. The latter is interpreted as a spreading center. At 168°30′E, the E-W lineations abut the N-S trending West Tikopia Ridge, which is interpreted as a major transform fault that offsets northward the spreading center from the Tikopia Ridge to the 9°30′ Ridge. The Hazel Holme Ridge is interpreted as an active and very young extensional zone or slow spreading ridge which crosscuts older oceanic crust and connects the N160° trending segment of the central spreading ridge with the southern tip of the northern New Hebrides backarc troughs. E-W trending magnetic lineations seem to be associated with the Hazel Holme Ridge but are not datable.

During the SEAPSO and STARMER French–Japanese joint projects, a detailed magnetic survey (Fig. 4.3) of the central part of the NFB was conducted. It allows us to refine identification of the magnetic anomalies and calculation of the spreading rate on the different segments during the past 3 m.y. (Auzende *et al.*, 1990c; Huchon *et al.*, 1994). The important features are the following.

1. An axial anomaly is identified all along the structural ridge axis. The width of this anomaly varies, giving spreading rates ranging from 50 to 82 mm/yr.

2. The J (Jaramillo) event is only clearly represented on the N-S segment. Its existence along the N15° and the southern part of the N160° segments is debatable. Based on the interpretation of the axial and J (Jaramillo) anomalies, the estimated spreading rate of the N160° segment has varied between 40 and 50 mm/yr, which are rates representative of intermediate rate spreading ridges. Along the entire N160° segment the present-day ridge axis is characterized by a morphology usually encountered at slow spreading ridges (Macdonald *et al.*, 1984). It is made up of a succession of deep grabens reaching more than 4000 m deep and bounded by steep 1000-m-high walls.

3. The anomalies 2 and 2A are clearly identified on both sides of the ridge axis, at least along the N-S and N15° segments. Along the southernmost N-S segment only anomaly 2 has been identified.

In the eastern part of the NFB, west of the Fiji Islands, the identification of magnetic anomalies (Fig. 4.8) also favors the existence of an active spreading center (Auzende *et al.*, 1994b). In the western part of the survey, corresponding to the propagating rift system, a well-defined anomaly is interpreted as anomaly 1. The width of this anomaly decreases from north to south. On both sides of the area, a magnetic lineation could be anomaly J (Jaramillo—1 Ma). The spreading rates calculated from these anomaly identifications are close to 40 mm/yr. The magnetic pattern exactly superimposes the structure. Between both axes, a large transverse E-W trending negative anomaly can be interpreted as the transform zone between the propagating rift and the southern rift (Hey *et al.*, 1986). This anomaly has no morphological expression. From the calculated spreading rate and the angles between the pseudofaults, the southward propagation velocity can be calculated. For an angle of 55° to 40°, as is observed north of 17°35′S, the propagation velocity is respectively 25 or 45 mm/yr. The tip of the propagator is characterized by a 20° angle with the pseudofault, implying an increase of the propagation velocity up to 100 mm/yr in the present phase. The age of this propagation could be related to the emplacement or the reactivation of the north Fiji fracture zone 1 to 1.5 m.y. ago (Lafoy *et al.*, 1990), resulting in the formation of the 16°50′S triple junction.

3. SEISMICITY

Gutenberg and Richter (1954) described isolated seismicity between the Tonga and New Hebrides arc major seismic zones. Sykes (1966) later succeeded in identifying a NE-SW trending seismic zone running from the southern tip of the New Hebrides arc to the center of the NFB. On the basis of seismic evidence, Sykes *et al.* (1969) suggested that the two triangular areas between the Tonga and New Hebrides arcs should be described as two different basins, the Lau and North Fiji basins. Chase (1971) extended this analysis and proposed a model including five microplates for the same area. The deep structure of the Lau and North Fiji basins was studied by Dubois (1971), Aggarwal *et al.* (1972), and Dubois *et al.* (1973). They showed the existence of a low-seismic-velocity zone in the upper mantle. Barazangi *et al.* (1974) demonstrated that this low-velocity zone was related to seismic-wave attenuation due to active spreading.

Crustal deformation in the NFB was addressed by Eguchi (1984), Hamburger and Isacks (1988), and Louat and Pelletier (1989), using a large number of shallow earthquake data and focal mechanism solutions from international catalogues. Despite discrepancies in their interpretations concerning the sense of active crustal motion, they provide a description of the distribution of shallow seismicity in the NFB and the major seismic lineaments (see following). Hamburger and Isacks (1988) claimed that there are no steady-state spreading centers in the NFB but only diffuse extensional zones in a wide strike-slip boundary between the Pacific and Australian major plates. In contrast, Louat and Pelletier (1989) tried to quantify the crustal motions along discrete spreading centers or transform faults, using the seismological and marine geological data.

Figure 4.13 shows the distribution of the shallow seismicity in the NFB (Louat and Pelletier, 1989). Earthquakes concentrate within certain areas delineating linear zones. Some of the seismic lines are associated with known structural features.

1. The north Fiji fracture zone (NFFZ) is clearly marked by a WSW-ENE trending seismic belt between 16° and 17°S from the central triple junction to the north of the Fiji Platform. Numerous focal mechanism solutions attest to E-W left-lateral strike-slip motion

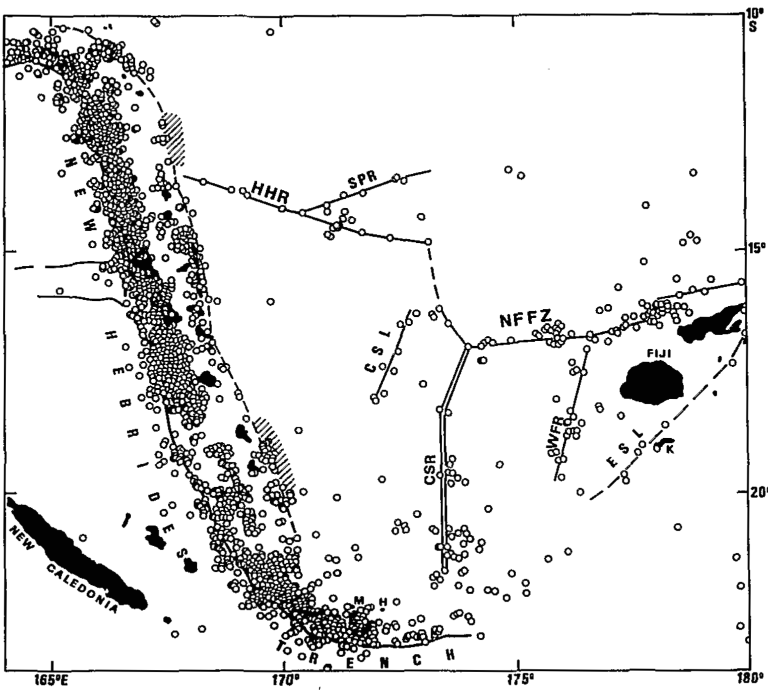

FIGURE 4.13. Shallow seismicity (0–70 km) in the NFB (after Louat and Pelletier, 1989). CSR: central spreading ridge; NFFZ: north Fiji fracture zone; WFR: West Fiji Ridge; HHR: Hazel Holme Ridge; SPR: South Pandora Ridge; CSL: central seismic lineament; ESL: eastern seismic lineament; K: Kandavu Island. See Louat and Pelletier (1989) for the data source.

along the NFFZ. However, events with normal fault solutions have occurred east of the 177°25′E pull-apart basin at 178°E and at the western end of the north Fiji fracture zone.

2. The West Fiji Ridge (WFR) coincides with a NNE-SSW trending seismic line located near 176°E, immediately west of the Fiji Platform between 17° and 20°S. Events with strike-slip or normal fault solutions occur along the west Fiji Ridge.

3. A WNW-ESE seismic belt correlates with the Hazel Holme Ridge between the New Hebrides backarc area and the northern tip of the N160°-trending segment of the central spreading ridge. Focal mechanism solutions indicate strike-slip faulting.

In contrast, the central spreading ridge, which is the major active spreading center of the basin, is almost unidentifiable with shallow seismicity. However, a few events cluster at particular areas: around 21°S at the tip of the southward propagating rift and at the offset of the axis, at 19°40′S where transverse volcanic alignments exist, around 18°10′S at the tip of the northward propagating rift, and between 16° and 17°S along the N160° trending segment. Events with strike-slip faulting solutions occur all along the central spreading ridge, but are especially concentrated at the 21°S ridge axis offset. However, one event with normal fault solution is located on the N160° segment.

Two seismic lineaments are observed in the basin where the bathymetry largely remains unknown (Louat and Pelletier, 1989): a NNE-SSW line (CSL) west of the central spreading ridge and characterized by pure normal faulting solutions, and a NE-SW line (ESL) between the Fiji Platform and Kandavu Island. Moreover, diffuse areas of seismicity are located in the southernmost part of the NFB and in the northeastern basin north of the NFFZ. All these seismic features indicate active crustal deformation which is still not understood.

4. HEAT FLOW DATA

Few heat flow measurements exist for the NFB. They all indicate high heat flow values (Sclater and Menard, 1967; Macdonald *et al.*, 1973; Halunen, 1979) over the entire basin, which is consistent with it being interpreted as a recent oceanic basin. At a smaller scale, two different provinces are distinguished. North of the Hazel Holme Ridge, the average heat flow value is 2.29 HFU; however, Halunen (1979) suggests that the heat flow is very low (0.88 HFU) if the New Hebrides arc volcanism effect is subtracted. These low values can be related to hydrothermal circulation or to the older age of this part of the NFB. South of the Hazel Holme Ridge, the values are higher with an average of 4 HFU. The relatively high heat flow values have been interpreted as indicative of the abnormally shallow depth of the NFB, called for this reason the North Fiji Plateau. In fact, the depths measured in the NFB are "normal" in terms of vertical evolution related to the age of the oceanic crust. Except in some peculiar areas such as the 16°50′S triple junction, the ridge crest depth varies from 2500 to 2800 m, which is the standard for mid-oceanic ridges (Sclater and Francheteau, 1970).

During the STARMER project a few heat flow measurements have been performed within the active rift valley by the submersibles *Nautile* and *Shinkai 6500*, close to the 16°50′S triple junction and in the area of the White Lady active hydrothermal site (see following). They all give low values (less than 1 HFU; Jòshima, pers. comm.) that are probably related to water circulation.

5. ROCK GEOCHEMISTRY

The compilation of the geochemical data collected along the North Fiji Basin spreading system between latitude 13°S and 22°S during the STARMER project (Eissen *et al.*, 1994; Lagabrielle *et al.*, 1994; Nohara *et al.*, 1994), in addition to all published data (Sinton *et al.*, 1985; Aggrey *et al.*, 1988; Auzende *et al.*, 1990a; Boespflug, 1990; Eissen *et al.*, 1990, 1991; Johnson and Sinton, 1990; Price *et al.*, 1990; Monjaret *et al.*, 1991; Sinton *et al.*, 1994), shows systematic geochemical variation along the different spreading segments. Crystal fractionation—controlled almost exclusively by olivine for the less fractionated lavas, or by plagioclase + olivine ± clinopyroxene for the most fractionated lavas—can explain part of the observed major element geochemical variations. However, the large ion lithophile elements (LILE), high field strength elements (HFSE), and rare earth elements (REE) contents of the basalts of the NFB as well as their isotopic compositions are strongly heterogeneous. Mixing of mantle sources must play a major role in order to explain the observed LILE, HFSE, REE, and isotopic variations. Thus, three different mantle sources have been identified in the NFB (Eissen *et al.*, 1994):

1. A typical depleted N-MORB source, producing basalts with flat patterns on N-MORB-normalized extended element variation diagrams (Fig. 4.14d), $1 < La/Nb < 2$ (Fig. 5.15; N-MORB field of Gill, 1981), and Sr- and Nd-isotopic ratios close to the Pacific MORB field (Fig. 4.14i).
2. An E-MORB- or OIB-related source giving basalts with a strong enrichment in HFSE, LILE, and LREE, on N-MORB-normalized extended element variation diagrams (Fig. 4.14a), $La/Nb < 1$ (Fig. 4.15; E-MORB field of Gill, 1981), and Sr- and Nd-isotopic ratios trending toward the intra-plate field (e.g. Samoan field in Fig. 4.14f).
3. A subduction-modified (or -related) mantle source, with basalts having generally a higher volatile content (Aggrey *et al.*, 1988), and a clear enrichment in HFSE, LILE, and LREE, on N-MORB-normalized extended element variation diagrams with a negative Nb anomaly indicating some subduction-related contamination (Fig. 4.14d), $La/Nb > 2$ (Fig. 4.14; orogenic field of Gill, 1981), and Sr- and Nd-isotopic ratios ranging from the Pacific MORB field to the New Hebrides arc field (Fig. 4.14h). These basalts derived from this source might also have been previously called BABB (Saunders and Tarney, 1984; Hawkins and Melchior, 1985; Sinton and Fryer, 1987).

The observed variations, reported as a function of their respective spreading segments, are as follows. Along the N-S segment, which also represents morphologically the most regular spreading ridge of the NFB, the magma source produces only basalts with N-MORB characteristics (Figs. 4.14d, 4.15). However, their isotopic compositions extend slightly over a range wider than the Pacific MORB field, with one trend toward the Samoan field and a weak trend toward the New Hebrides field (Fig. 4.14i). Along the N15° segment the three sources coexist, giving a wide range of geochemical signatures for the basalts collected (Fig. 4.15). Their mixing results in a large number of transitional compositions giving patterns of E-MORB types (Fig. 4.14c). Their isotopic compositions are essentially similar to the more Sr radiogenic of the Pacific MORB with two additional groups having, respectively, an OIB- and a subduction-related trend (Fig. 4.14h). The source mixing transitional toward OIB (hot-spot-related) increases northward from 18°20′S to 12°S, as the Rotuma–Samoan hot-spot lineament is approached. Thus, along the N160° segment, the three sources still coexist, but the influence of the OIB source increases, whereas the influence of the subduction-related source decreases (Figs. 4.14b and 4.15). It is particularly

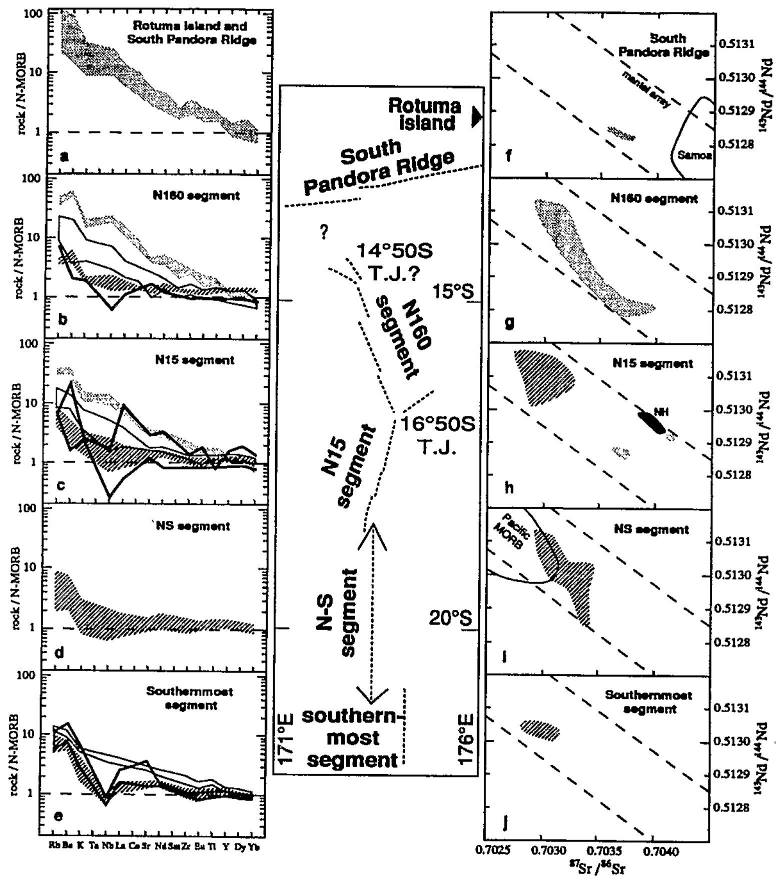

FIGURE 4.14. Incompatible elements and isotopic variations of the North Fiji Basin basalts as a function of a schematic spreading segmentation (central sketch); (a–e) N-MORB-normalized extended element variation diagrams (normalization values after Sun and McDonough, 1989); (f–j) variations of $^{87}Sr/^{86}Sr$ with $^{143}Nd/^{144}Nd$ (Pacific MORB field after Boespflug, 1990; Samoan field after Wright and White, 1987; NH: New Hebrides 1 field after Briqueu *et al.*, 1994). Light gray field: OIB-related source; dark gray field: N-MORB source; thin lines field: transitional toward OIB (or E-MORB) source; heavy lines field (with negative Nb anomaly): subduction related source.

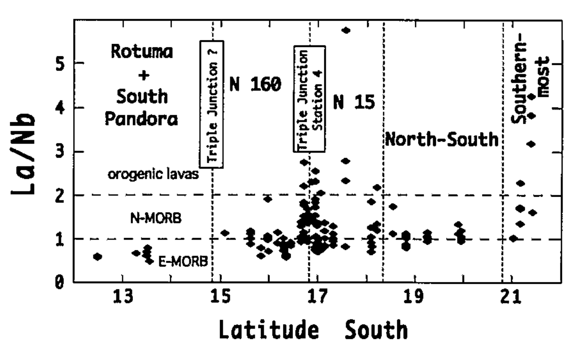

FIGURE 4.15. La/Nb along-strike variations of the North Fiji Basin basalts as a function of the latitude of the sampling site.

well marked on the isotopic composition diagram (Fig. 4.14g) where all the compositions spread between the Pacific MORB and the Samoan fields. Along the Pandora–Rotuma Ridge, only the OIB-derived lava type is present, the eventual contribution from other sources being completely diluted (Figs. 4.14a, 4.14f, 4.15). Mixing calculations based on incompatible elements involving OIB and N-MORB sources show that the OIB source contribution is between 50% and 80% for the Rotuma–Pandora Ridge lavas and is lower than 25% for the N160° and N15° segments (Eissen *et al.*, 1994). On the southernmost segment (N174°E), N-MORB are present, but the dying subduction along the Hunter Ridge still influences several basalt compositions, which show a significant subduction-related contamination with negative Nb anomalies and high volatiles content. A weak E-MORB source contribution is also present in several others and may be related to subducted-OIB seamounts from the South Fiji Basin (Fig. 4.14e, 4.14j). However, no significant isotopic variations are observed along this segment (Fig. 4.15).

Thus, the geochemistry of the NFB magma sources is directly influenced by the surrounding active or dead subduction zones and the regional OIB (or hot-spot)-related sources. The magma genesis is dominantly controlled by magma production along the spreading system, resulting in the dominance of N-MORBs. However, this source mixes to a various extent with the two sources mentioned previously. In the entire northern NFB many basalts result from the mixing of an N-MORB and a OIB source, similar to transitional alkalic lavas from oceanic intraplate magmatism. This source is related either to the Samoan lineament (Wright and White, 1987) or to the Fiji Platform (Gill, 1984) or even to the Wallis lineament (Price *et al.*, 1991). Similarly, if the subduction-related contamination along the 174°E segment is directly linked to the dying subduction at the southern end of the New Hebrides arc, the presence of perceptible subduction-related geochemical characteristics in basalts from the central NFB, 500 km away from the active subduction zone, is more questionable. This influence results in fact from the partial melting of an upper mantle source that was affected by subduction contamination during the clockwise rotation of the New Hebrides arc leading to the opening of the NFB during the past 10 m.y. (Malahoff *et al.*, 1982a; Auzende *et al.*, 1988a) and is no longer directly linked to the presently active subduction.

6. SULFIDE DEPOSITS

Since the beginning of the SEAPSO and STARMER projects, two main hydrothermal sulfide deposit fields have been explored by *Nautile* in 1989 (Auzende *et al.*, 1991b) and *Shinkai 6500* in 1991 (Auzende *et al.*, 1992a) in the vicinity of the 16°50′S triple junction (Lafoy *et al.*, 1987, 1990). The first (named "White Lady") at 16°59′S and the second (named "Père Lachaise") at 16°58′S were both discovered during the *Nautile* dives in 1989.

The main structural features, which characterize the 2-km-wide, 100–150-m-deep rift valley of the NFB in the White Lady area, are steep fault scarps associated with open fissures. Fissures a few meters long and a few centimeters to 1-m wide are commonly observed on the seafloor and on the terraces adjacent to the fault scarps. The fault trend is parallel to the main trend of the central spreading ridge, N10° to N20° (Fig. 4.16). The White Lady chimney (Figs. 4.16 and 4.17) is located on the top of a 6–7-m-high, 50-m-diameter mound composed of sulfides and oxides. The chimney bifurcates and is

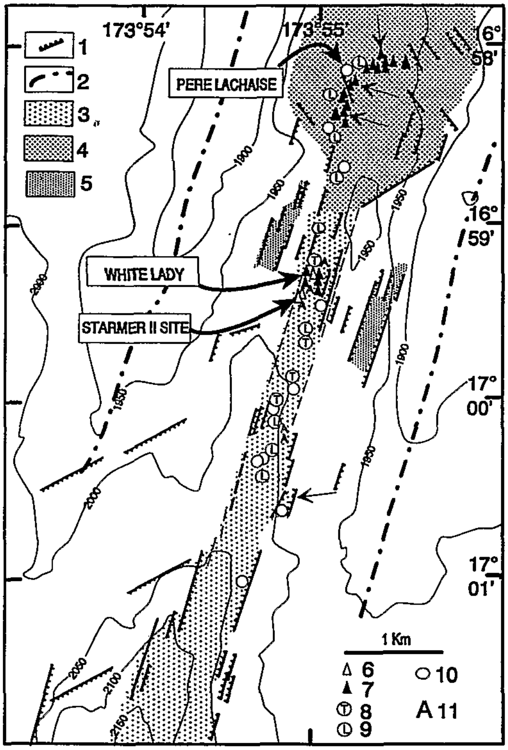

FIGURE 4.16. Detailed structural map of the axial graben close to 17°S. Location of the active hydrothermal sites (White Lady and STARMER) and major sulfides deposit (Père Lachaise) (after Bendel *et al.*, 1993). 1: normal faults; 2: crest; 3: main axial graben; 4: intersection zone; 5: secondary graben; 6: active hydrothermal site; 7: fossil chimneys; 8: temperature anomalies; 9: lava lakes; 10: hydrothermal oxydes staining; 11: mussels and gastropods colonies. The small arrows indicate the sampling areas out of the White Lady site.

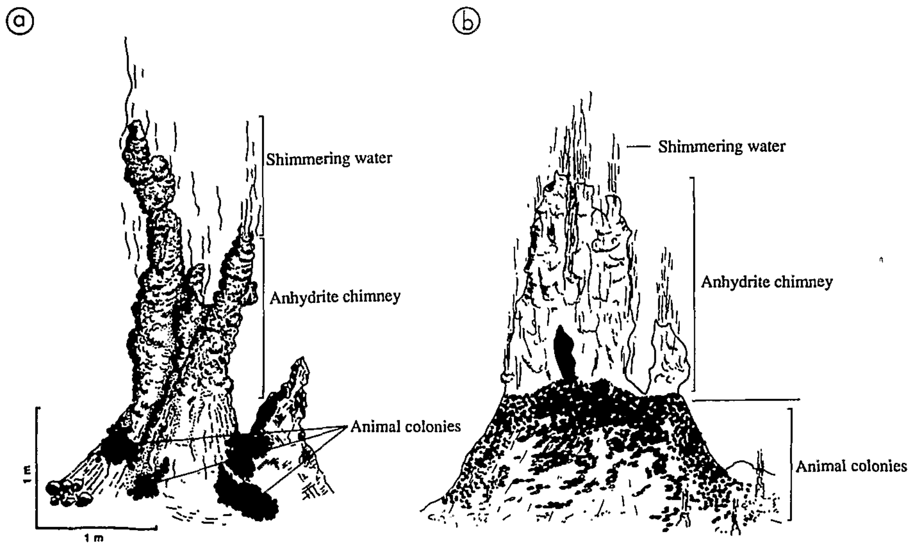

FIGURE 4.17. Artistic view of the White Lady evolution from (a) 1989 and (b) 1991 (after Auzende *et al.*, 1992a).

composed exclusively of anhydrite. It expels shimmering 285°C water, which is poor in particulates. At the foot of the main chimney, six secondary vents expelling the same transparent water are colonized by gastropods, mussels, crabs, and cirripeds. In 1991, six *Shinkai 6500* dives were devoted to the study of the White Lady and of the surrounding active hydrothermal sites. The present-day condition of the White Lady can be summarized as follows: the anhydrite chimney currently comprises a massive 2-m-high, 2-m-diameter main conduit and a 1.5-m-high, 10-cm-diameter secondary chimney. These vents expel the same shimmering water, but the flux is about twice that of two years ago. The measured temperature is 265°C, 20°C less than the measured temperature in 1989. Finally, significant changes (Fig. 4.17) have been observed for the colonies of living fauna. They are in all cases more numerous, and their territories are expanding toward the top of the mound. The sulfates, oxides, and sulfides have been studied in great detail by Bendel (1993) and Bendel *et al.* (1993), who deduced from geological observations and mineralogical study four stages in the evolution of the White Lady site. The sulfide spires are formed in the first stage by mixing of hydrothermal fluid with seawater. The sulfide mound and the maturation of sulfides reflect the second stage. Copper-rich massive sulfides are precipitated at the core of the mound. During the third stage the sulfides are tectonically brecciated, and the resulting fissures are filled with amorphous silica, talc, and barite. The fourth stage corresponds to anhydrite precipitation related to the present-day activity at the top of the sulfide mound.

The Père Lachaise site is characterized by the disappearance of the axial graben and the increasing width of the domain. This area, close to the 16°50′S triple junction, exhibits three sets of normal fault and fissures trending N15°, N140–150°, and N60°. The explored fossil hydrothermal field consists of several tens of individual spires growing directly on basalt scattered over a 2-km × 2-km surface. The deposits sampled from the Père Lachaise site indicate the same compositions as are observed on the White Lady mound. The absence of a massive mound in this area is interpreted as the result of the conjunction of the three directions of faulting, which creates a zone of high porosity where hydrothermal discharge is dispersed over a large area (Bendel *et al.*, 1993).

7. WATER SAMPLING

The first significant water samples on the ridge axis were taken in 1985 during the SEAPSO III cruise (Auzende *et al.*, 1988a) and the Papatua cruise in 1986 (Craig, 1986). Other water samplings have been conducted on the northern part of the NFB ridge during the Moana Wave cruise in 1987. They indicate hydrothermal activity around the South Pandora Ridge (Kroenke *et al.*, 1987).

During the SEAPSO III cruise, seven hydrocasts were taken on the axis between 16°S and 20°S. Four of these indicate significant methane and manganese anomalies close to the seafloor; two hydrocasts are located at the junction of the N-S and N15° segments and the other two are on the N160° segment close to the 16°50′S triple junction. These last hydrocasts show anomalies 10 times higher than background level for the deep Pacific water. During the STARMER project, hydrocasts were taken about every 20 miles all along the ridge axis. They demonstrate the quite constant distribution of the hydrothermal activity along the spreading ridge axis.

In situ sampling was conducted during the STARMER *Nautile* cruise (1989) and the

Shinkai 6500 cruise (1991) on the White Lady active site at 17°S in the triple junction area (Auzende *et al.*, 1991b). The main results can be summarized as follows (Grimaud *et al.*, 1991; Ishibashi *et al.*, 1994): the samples were collected with conventional titanium syringes by *Nautile* or with a pumping system by *Shinkai 6500*. In total, 16 samples were taken on the White Lady site. Their compositions range from a few percent hydrothermal water to nearly pure 285°C temperature fluids. The elemental concentrations show linear trends on element versus Mg diagrams. All the element concentrations of the parent end member are significantly lower than all other hydrothermal systems. Chloride (255 mmol/kg) and sodium (210 mmol/kg) have especially low concentrations compared with fluids collected on the East Pacific Rise (EPR), Juan de Fuca Ridge, Galapagos Ridge (von Damm and Bischoff, 1987) and Mid-Atlantic Ridge (Campbell *et al.*, 1988). The only similar fluids have been sampled in the Ashes vent field on the Juan de Fuca Ridge (Massoth *et al.*, 1989; Butterfield *et al.*, 1990). In spite of these low concentrations the characteristic elemental ratios K/Na and Ca/Sr are close to the values usually found in other hydrothermal systems (von Damm and Bischoff, 1987).

8. DISCUSSION AND CONCLUSION

The evolution of the NFB, located between the opposed New Hebrides and Tonga subduction zones, results from variation in the relative motions of the Australian and Pacific plates. At a large scale the NFB can be interpreted as a deformation zone at the boundary of the two plates. Depending on the geometry of the boundary, the shortening between the plates will be accommodated by compressive stresses such as along New Hebrides and Tonga trenches or by strike-slip motion such as in the northern part of the basin. The geometry of the ridge axis, its segmentation, and its changes of direction are controlled by this relative motion.

8.1. Hectokilometric, Decakilometric, and Kilometric Ridge Segmentation

The precise mapping of the central spreading ridge illustrates different scales of segmentation. At a large scale, five main segments can be considered. Their length varies from about 140 km for the southernmost N-S segment to more than 280 km for the N-S segment. Although the spreading rate is intermediate all along the central spreading ridge, ranging from 50 mm/yr on the N160° and N15° segments to 80 mm/yr on the N-S segment, the segments show very different morphologies. The N-S and N15° segments' morphology is typical of EPR fast-spreading-type morphology (Fig. 4.4) with a central dome 8 km wide cut in its axial part by a graben 50 m to several hundred meters wide and 50 m deep. In contrast, the N160° segment is characterized by an 8-km-wide, 1000-m-deep graben occupied in its axial part by a neovolcanic zone (Fig. 4.4). This morphology is typical of slow-spreading MAR-type morphology. The conclusion drawn from these observations is that there is not a unique correlation between the ridge morphology and the spreading rate. It is also necessary to take into account the magmatic budget of each area and its geodynamic context. The drastic change of morphology north and south of the 16°50′S triple junction suggests that the triple junction area constitutes a magmatic supply boundary between the N15° segment, characterized by significant volcanic construction, and the amagmatic extension of the N160° segment.

Within each major segment, segmentation at the scale of 10 s of kilometers is observed. These subsegments are limited by offsets, OSCs, and propagating rifts as described on the EPR (Macdonald, 1983) and as illustrated in Fig. 4.3. The average lengths of these intermediate subsegments varies from 40 km on the N-S segment to more than 60 km on the N160° segment.

Segmentation at a scale of a kilometer has also been documented on the N-S segment around 19°S by the *in situ* exploration with *Nautile* and *Shinkai 6500* (Ondréas *et al.*, 1993; Gracia-Mont *et al.*, 1994). The active accretion is located in tectonic grabens a kilometer long and tens of meters wide separated by kilometer-wide magmatic saddles between the grabens. The active hydrothermal sites are located in the grabens, whereas very fresh magmatic edifices are observed on the saddles.

8.2. Unusual Tectonic Features

One of the characteristics of spreading in the NFB is the existence all along the ridge axis of unusual tectonic features such as propagating rifts, OSC, offsets, and others, representative of the complex geodynamic environment of the basin. At a global scale the NFB can be considered as a megashear zone at the boundary between the Australian and Pacific plates (Hamburger and Isacks, 1988). The effect of these permanent shear stresses applied on the whole basin is the deformation of the spreading ridge. This deformation is accommodated by changes of morphology and migration of the ridge axis with initiation of triple junctions (examples of 16°50′S and 14°50′S triple junctions) and ridge propagation (northward propagation of the N-S segment at 18°10′S, southward propagation of the N-S segment at 20°30′S) and activation of major transform faults (north Fiji fracture zone, central fracture zone, and south Fiji fracture zone) (Fig. 4.18).

Also, probably as a result of the geodynamic environment, the accretion south of the north Fiji fracture zone is distributed on two parallel active spreading ridges, the central spreading ridge and the West Fiji Ridge, propagating at a large scale, respectively to the north and to the south (Auzende *et al.*, 1993, 1994b). Since at least 1.5 to 1 Ma, this twin-spreading-ridge system isolates an intermediate West Fiji microplate between the central spreading ridge and the West Fiji Ridge (Fig. 4.18). The same phenomenon is observed for the Easter (Francheteau *et al.*, 1987; Larson *et al.*, 1992) and Juan Fernandez microplates. The spreading rates on both ridges vary, increasing from south to north on the West Fiji Ridge and from north to south on the central spreading ridge. The sum of spreading rates is close to 100 mm/yr all along the N-S oceanic crust created during the last 1 to 1.5 m.y.

8.3. Petrology and Geochemistry

The compilation of all the geochemical data available for the basalts of the NFB shows that low-pressure crystal fractionation controls the major element geochemistry, and mantle source heterogeneities and their mixing dominantly control the LILE, HFSE, and REE patterns and isotopic compositions of these basalts. The dominant magma of this backarc basin is an N-MORB type, producing basalts very similar to those emplaced along the most classical intermediate-rate mid-oceanic spreading centers. But other geochemical signatures, representative of the local upper mantle geochemistry, are observed: (1) an OIB source, similar to transitional alkalic lavas from oceanic intraplate magmatism; its influence increases northward from 18°20′S to 12°S, this lava type being the only one present

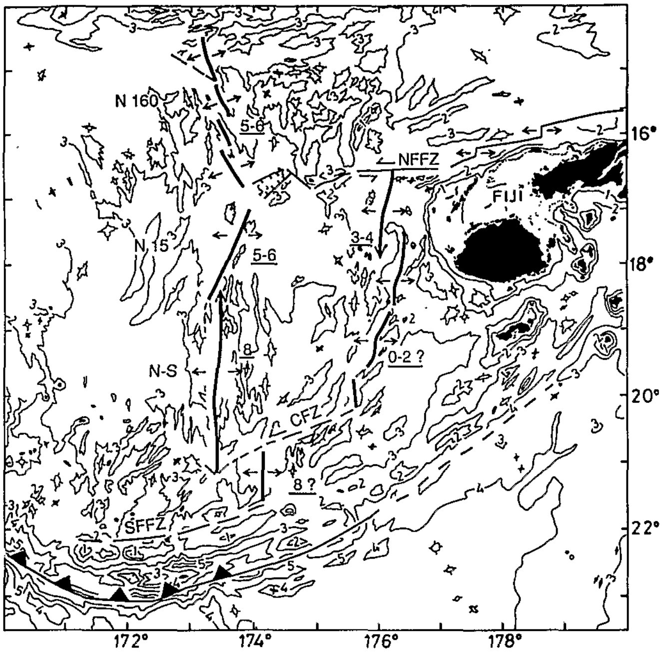

FIGURE 4.18. Kinematic sketch of the twin ridges (central spreading ridge and the West Fiji Ridge) with simplified bathymetry. NFFZ: north Fiji fracture zone; CFZ: central Fiji fracture zone; SFFZ: south Fiji fracture zone; N-S, N15 and N160: the different segments of the main central spreading ridge. *5–6*: spreading rate calculated from magnetic data. *0–2?*: inferred spreading rate in cm/yr. The arrows at the tip of ridge segments indicate the direction of propagation (after Auzende *et al.*, 1994b).

along the Rotuma–Pandora Ridge; and (2) a source that was affected by subduction contamination from the New Hebrides subduction, with a clear enrichment in incompatible elements, a negative Nb anomaly, and a high loss on ignition (LOI). This contamination with variable arc affinity, which affected the entire NFB upper mantle, was left behind after the clockwise rotation of this arc, as a result of the opening of the NFB. This subduction-related material was then recycled during partial melting of the NFB upper mantle beneath the central spreading axis.

8.4. Hydrothermal Activity: Water Chemistry and Sulfides

The explored hydrothermal active sites of the NFB central spreading ridge are probably only representative of a few percent of the hydrothermal activity. The hydrocasts taken all along the ridge axis suggest a widespread activity with the indication in some places of a very strong but unstable activity. For example, the 19°S "megaplume" (Nojiri *et al.*, 1989) discovered during the *Kaiyo* cruise in 1987 was extinct two years later when attempts were made to sample it again.

One of the main characteristics of the NFB ridge axis hydrothermal waters sampled by *Nautile* and *Shinkai 6500* on the White Lady site is their low salinity, which suggests that fluids have undergone phase separation (Grimaud *et al.*, 1991; Ishibashi *et al.*, 1994). Such a phase separation would result in the formation of one vaporlike phase with low salinity and one liquid-like phase with high salinity (brine). Dissolved species will be depleted in the vapor, but phase separation will not significantly modify the elemental ratios as observed in the White Lady waters. To conclude, the NFB hydrothermal waters could result from three-component mixing of normal hydrothermal water, low-salinity fluid from condensed vapor, and brine.

Concerning the sulfides, the analysis of the White Lady site deposits succession implies three different hydrothermal episodes (Bendel, 1993; Bendel *et al.*, 1993): (1) The first episode is characterized by deposition of Cu, Fe, and Zn-rich sulfides and implies that a hot (more than 300°C) water was being expelled. This episode is close to the mid-oceanic ridge type. (2) The second hydrothermal episode produced opal, barite, and talc precipitates. It certainly occurs after a tectonic event which was responsible for the sulfides mound brecciation. This tectonic event caused the fluids to become more oxidized with temperatures ranging from 150°C to 300°C, depending on subsurface mixing. (3) The third hydrothermal episode only produced anhydrite and minor opal and talc. This deposit was associated with low elemental abundances in the expelled water and could be, as suggested by Grimaud *et al.* (1991) and Ishibashi *et al.* (1994), the result of a phase separation after boiling near the surface. The succession of these three hydrothermal phases results in a great instability of the hydrothermal system over a short period of time (less than 1 m.y.). This instability could be related to the tectonic events affecting the area, especially the intense tectonic fracturing associated with the 16°50′S triple junction.

8.5. Evolution of the Basin

The recent data acquired on the northern and the northwestern parts of the NFB (especially those of Pelletier *et al.*, 1988, 1993a,b) allow construction of a previously proposed geodynamical evolution model (Auzende *et al.*, 1988b) to be completed. The evolution of the NFB is illustrated by the six cartoons of Fig. 4.19.

1. At 12 Ma the Vitiaz–New Hebrides–Fiji–Lau–Tonga arc split and NFB rifting started with the change of subduction polarity from the Vitiaz to the New Hebrides system. The main part of the initial arc remained on the southern side of the spreading axis.
2. Spreading along a NW-SE axis was synchronous with the clockwise rotation of the New Hebrides arc and the anticlockwise rotation of the Fiji Platform. The initial axis located north of the Fiji Platform jumped southward between the New Hebrides and Fiji. The crust created during this stage is mainly located in the western basin.
3. At 7 Ma the NW-SE spreading axis stopped and was replaced by an E-W trending spreading center from the northwestern tip of the basin to the north of the Fiji Platform. This center corresponds to the 9°30′S, Tikopia, and proto–south Pandora ridges. This opening induced a new subduction zone along the southern limit of the NFB.
4. A triple junction was active around 3 Ma (anomaly 2A) between the former E-W axis and the newly created N-S-trending spreading center. At this stage there was a major change in the stress direction from N-S to E-W. This period was synchronous with the beginning of spreading in the Lau Basin.
5. Around 1.5 Ma the opening along the E-W axis was reorganized by the development of the north Fiji fracture zone along the Fiji Platform up to the N-S spreading axis, creating the 16°50′S triple junction. The left-lateral strike-slip motion along the north Fiji fracture zone induced the change of the direction of the N-S axis at the 16°50′S triple junction. The West Fiji and Hazel Holme ridges developed to accommodate strike-slip motion along the north Fiji fracture zone.

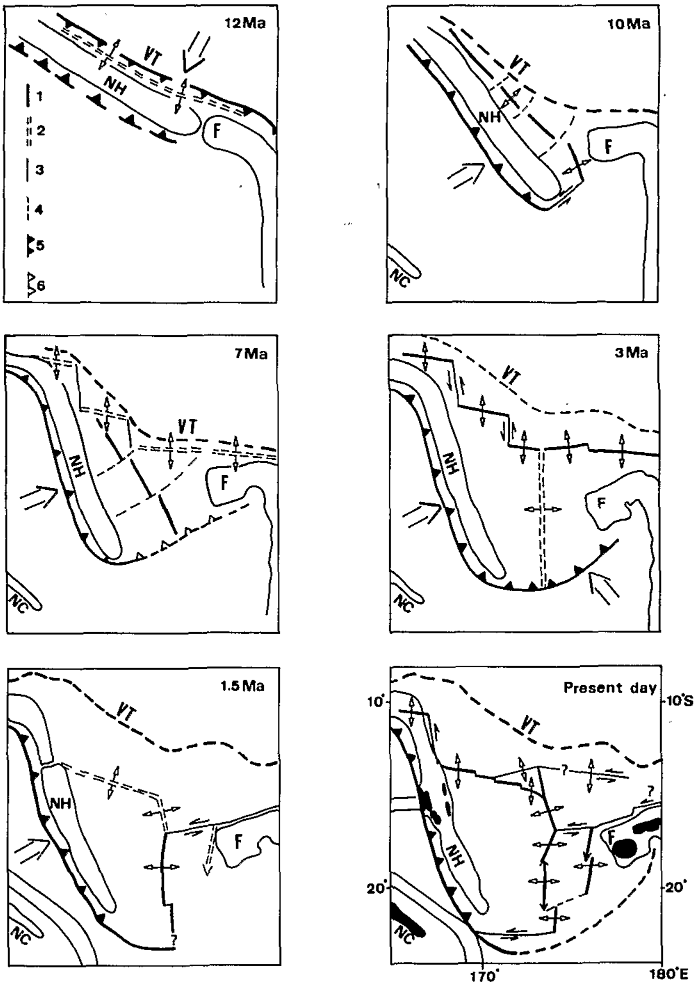

FIGURE 4.19. Geodynamic evolution of the North Fiji Basin. See text for explanation. 1: active ridge axis; 2: incipient ridge axis; 3: transform fault; 4: flowlines; 5: active subduction zone; 6: incipient subduction zone. VT: Vitiaz Trench; NH: New Hebrides arc; F: Fiji Platform; NC: Nouvelle-Calédonie.

6. At present, the spreading south of the north Fiji fracture zone is distributed along the parallel central spreading ridge and West Fiji Ridge isolating an intermediate microplate. To the south, the southernmost spreading axis is connected to the New Hebrides Trench by a large left-lateral strike-slip fault. North of the 16°50′S triple junction, opening occurs along the N160° segment and the Hazel Holme Ridge. The Santa Cruz Trough, which crosscuts the northernmost part of the New Hebrides arc, could be linked to the Hazel Holme spreading system. Crustal motion probably occurs in the north and the northeastern part of the NFB along the South Pandora Ridge and its eastern prolongation, interpreted either as a slow spreading ridge or a strike-slip fault. This lineament is connected with the N160°–Hazel Holme system by the 14°50′S triple junction.

Finally the opening of the NFB can be divided into three major stages: an opening in a NE-SW direction from 12 to 7 Ma, an opening in a N-S direction from 7 to 3 Ma, and an opening in an E-W direction from 3 Ma to the present day. The triangular shape of the basin results from these three successive spreading phases. Since the beginning of the creation of the NFB, the location of the successive spreading centers has migrated southward to accompany the migration of the New Hebrides arc.

Acknowledgments

We thank all the scientific parties and the ships and submersibles crews involved in the studies of NFB during the SEAPSO, EVA, and STARMER projects. We thank Thomas Brocher, Brian Taylor, and an anonymous reviewer for their constructive comments and for their help in improving our English. J. Butscher and J. Perrier are thanked for the preparation of the illustrations.

REFERENCES

Aggarwal, Y. P., Barazangi, B., and Isacks, B. 1972. P and S travel times in the Tonga–Fiji region: A zone of low velocity in the uppermost mantle behind the Tonga Island arc, *J. Geophys. Res.* **77**:6427–6434.

Aggrey, K. E., Muenow, D. W., and Sinton, J. M. 1988. Volatile abundances in submarine glasses from the North Fiji and Lau backarc basins, *Geochim. Cosmochim. Acta* **52**:25401–2506.

Alteris (de), G., Ruellan E., Auzende J. M., Ondréas H., Bendel V., Gracia-Mont E., Lagabrielle Y., Huchon P., and Tanahashi M. 1993. Propagating rifts in the North Fiji Basin (Southwest Pacific), *Geology* **21**:583–586,

Auzende, J. M., Bendel, V., Fujikura, K., Geistdoerfer, P., Gracia-Mont, E., Joshima, M., Kisimoto, K., Mitsuzawa, K., Murai, M., Nojiri, Y., Ondreas, H., Pratt, C., and Ruellan, E. 1992a. Résultats préliminaires des plongées du "Shinkai 6500" sur la dorsale du Bassin Nord-Fidjien (SW Pacifique)–STARMER, *C.R. Acad. Sci. Paris* **314**(II):491–498.

Auzende, J. M., Boespflug, X., Bougault, H., Dosso, L., Foucher, J. P., Joron, J. L., Ruellan, E., and Sibuet, J. C. 1990a. From intraoceanic extension to mature spreading in back arc basins: Examples from the Okinawa, Lau and North Fiji Basin, Actes du Colloque Tour du Monde Jean Charcot, *Oceanol. Acta* **10**:153–163.

Auzende, J. M., Eissen, J. P., Caprais, M. P., Gente, P., Gueneley, S., Harmegnies, F., Lagabrielle, Y., Lapouille, A., Lefèvre, C., Maillet, P., Mazé, J.P., Ondréas, H., Schaaf, A., and Singh, R. 1986a. Accrétion océanique dans la partie méridionale du bassin Nord-Fidjien: Résultats préliminaires de la campagne océanographique SEAPSO III du N.O. Jean Charcot (décembre 1985), *C.R. Acad. Sci. Paris* **303**:93–98.

Auzende, J. M., Eissen, J. P., Lafoy, Y., Gente, P., and Charlou, J. L. 1988a. Seafloor spreading in the North Fiji Basin (Southwest Pacific), *Tectonophysics* **146**:317–351.

Auzende, J. M., Gracia-Mont, E., Bendel, V., Huchon, P., Lafoy, Y., Lagabrielle, Y., de Alteris, G., and Tanahashi, M. 1994a. A possible triple junction at 14°50′S on the North Fiji Basin Ridge (Southwest Pacific), *Mar. Geol.* **116**:25–36.

Auzende, J. M., Gracia-Mont, E., Bendel, V., Lafoy, Y., Lagabrielle, Y., Okuda, Y., and Ruellan, E. in press. Amagmatic extension at intermediate spreading ridge (North Fiji Basin), in *Oceanic Lithosphere*, Special Issue (P. Kapezinskhas, ed.), Wiley, New York.

Auzende, J. M., Hey, R. N., Pelletier, B., Lafoy, Y., and Lagabrielle, Y. 1993. Propagation d'une zone d'accrétion à l'est de la dorsale du bassin Nord Fidjien (SW Pacifique), *C.R. Acad. Sci. Paris* **317**(II):671–678.

Auzende, J. M., Honza, E., Mazé, J. P., and the STARMER Group. 1992b. Comments on the Seabeam map of the North Fiji Basin Ridge between 16°10′S and 21°40′S, *Ofioliti* **17**(1):43–53.

Auzende, J. M., Honza, E., and the STARMER Group. 1990b. Bathymetric map of the North Fiji Basin Ridge between 16°10′S and 21°40′S, published by IFREMER and STA Japan, six colored sheets edited by Beicip, Paris.

Auzende, J. M., Lafoy, Y., and Marsset, B. 1988b. Recent geodynamic evolution of the North Fiji Basin (SW Pacific), *Geology* **16**:925–929.

Auzende, J. M., Lagabrielle, Y., Schaaf, A., Gente, P., and Eissen, J. P. 1986b. Tectonique intra-océanique décrochante à l'ouest des îles Fidji (Bassin Nord Fidjien). Campagne SEAPSO III du N.O. Jean Charcot, *C.R. Acad. Sci. Paris* **303**:241–246.

Auzende, J. M., Okuda, Y., Bendel, V., Ciabrini, J. P., Eissen, J. P., Gracia, E., Hirose, K., Iwabushi, Y., Kisimoto, K., Lafoy, Y., Lagabrielle, Y., Marumo, K., Matsumoto, T., Mitsusawa, K., Momma, H., Mukai, H., Nojiri, Y., Okuda, Y., Ortega-Osorio, A., Ruellan, E., Tanahashi, M., Tupua, E., and Yamaguchi, K. 1991a. Propagation "en échelon" de la dorsale du Bassin Nord Fidjien entre 16°40 et 14°50S (Yokosuka 90–STARMER), *C.R. Acad. Sci. Paris* **312**(II):1531–1538.

Auzende, J. M., Pelletier, B., and Lafoy, Y. 1994b. Twin active spreading ridges in the North Fiji Basin (S.W. Pacific), *Geology* **22**:63–66.

Auzende, J. M., and the STARMER Group. 1990c. Active spreading and hydrothermalism in North Fiji Basin (SW Pacific). Results of Japanese–French cruise *Kaiyo 87*, *Mar. Geophys. Res.* **12**:269–283.

Auzende, J. M., Urabe, T., Bendel, V., Deplus, C., Eissen, J. P., Grimaud, D., Huchon, P., Ishibashi, J., Joshima, M., Lagabrielle, Y., Mevel, C., Naka, J., Ruellan, E., Tanaka, T., and Tanahashi, M. 1991b. In situ geological and geochemical study of an active hydrothermal site on the North Fiji Basin Ridge, *Mar. Geol.* **98**:259–269.

Barazangi, M., Isacks, B. L., Dubois, J., and Pascal, G. 1974. Seismic wave attenuation in the upper mantle beneath the Southwest Pacific, *J. Geophys. Res.* **76**:8493–8516.

Bendel, V. 1993. Cadre gèologique et composition des minéralisations hydrothermales en contexte arrière-arc: exemple de la dorsale du Bassin Nord Fidjien, Thèse Université Brest, France.

Bendel, V., Fouquet, Y., Auzende, J. M., Lagabrielle, Y., Grimaud, D., and Urabe, T. 1993. Metallogenesis at a Triple Junction system: The White Lady hydrothermal field (North Fiji Back-Arc Basin, SW Pacific), *Economical Geol.* **88**:2237–2249.

Boespflug, X. 1990. Evolution géodynamique et géochimique des bassins arrière-arcs. Exemples des bassins d'Okinawa, de Lau et Nord-Fidjien, Thèse, Université Brest, France.

Briqueu, L., Laporte, C., Crawford, A., Hasenaka, T., Baker, P., and Coltorti, M. 1994. Temporal magmatic evolution of the Aoba basin–central New Hebrides Island Arc: Pb, Sr and Nd isotopic evidence for the coexistence of two mantle components beneath the arc, in *Proc. ODP, Sci. Results*, 134 (H. G. Greene, J.-Y. Collet, L. B. Stokking *et al.*, eds.), pp. 393–401, Ocean Drilling Program, College Station, TX.

Brocher, T. M. 1985, On the formation of the Vitiaz Trench lineament and North Fiji Basin, in *Investigations of the Northern Melanesian Borderland* (T. M. Brocher, ed.), pp. 13–34, Circum-Pacific Council for Energy and Mineral Resources, Houston, TX, Earth Science Series, Vol. 3.

Brocher, T. M., and Holmes, R. 1985. The marine geology of sedimentary basins south of Viti Levu, Fiji, in *Investigations of the Northern Melanesian Borderland* (T. M. Brocher, ed.), pp. 123–138, Circum-Pacific Council for Energy and Mineral Resources, Houston, TX, Earth Science Series, Vol. 3.

Butterfield, D. A., Massoth, G. J., McDuff, R. E., Lupton, J. E., and Lilley, D. 1990. Geochemistry of hydrothermal fluids from Axial Seamount Hydrothermal Emissions Study vent field, Juan de Fuca Ridge: Subseafloor boiling and subsequent fluid-rock interaction, *J. Geophys. Res.* **95**:12,895–12,921.

Campbell, A. C., *et al.* 1988. Chemistry of hot springs on the Mid-Atlantic Ridge, *Nature* **335**:514–518.

Cande, S. C., and Kent, D. V. 1992. A new geomagnetic polarity time scale for the late Cretaceous and Cenozoic, *J. Geophys. Res.* **97**(B10):13,917–13,951.

Charvis, P., and Pelletier, B. 1989. The northern New Hebrides backarc troughs: History and relation with the North Fiji Basin, *Tectonophysics* **170**:259–277.

Chase, C. G. 1971. Tectonic history of the Fiji Plateau, *Geol. Soc. Am. Bull.* **82**:3087–3110.

Cherkis, N. Z. 1980. Aeromagnetic investigations and sea floor spreading history in the Lau basin and the northern Fiji Plateau, in *Symposium on Petroleum Potential in Island Arcs, Small Basins, Submerged Margins and Related Areas* (W. J. Clark, ed.), United Nations, ESCAP, CCOP/SOPAC, Technical Bull. **3**:37–45.

Craig, H. 1986. Papatua 86: A grand tour of the Havre Trough and the Lau, North Fiji, Woodlark and Manus Basins, *Eos* **67**:378.

Daniel, J. 1982. Morphologie et structures superficielles de la partie sud de la zone de subduction des Nouvelles-Hébrides, in *Contribution à l'étude géodynamique du Sud-Ouest Pacifique*, Equipe de Géologie- Géophysique du Centre ORSTOM de Nouméa, Travaux et Documents de l'ORSTOM **147**:39–60.

Dubois, J. 1971. Propagation of P waves and Rayleigh waves in Melanesia: structural implications, *J. Geophys. Res.* **76**:7217–7240.

Dubois, J., Launay, J., Récy, J., and Marshall, J. 1977. New Hebrides Trench: Subduction rate from associated lithospheric bulge, *Can. J. Earth Sci.* **14**:250–255.

Dubois, J., Pascal, G., Barazangi, M., Isacks, B. L., and Oliver, J. 1973. Travel times of seismic waves between the

New Hebrides and Fiji Islands: A zone of low velocity beneath the Fiji Plateau, *J. Geophys. Res.* **78**:3431–3436.

Eguchi, T. 1984. Seismotectonics of the Fiji Plateau and Lau Basin, *Tectonophysics* **102**:17–32.

Eissen, J. P., Lefèvre, C., Maillet, P., Morvan, G., and Nohara, M. 1991. Petrology and geochemistry of the central North Fiji Basin spreading center (SW Pacific) between 16°S and 22°S, *Mar. Geol.* **98**:201–239.

Eissen, J. P., Morvan, G., Lefèvre, C., Maillet, P., Urabe, T., Auzende, J. M., and Honza, E. 1990. Pétrologie et géochimie de la zone d'accrétion du centre du bassin Nord Fidjien (SW Pacifique), *C.R. Acad. Sci. Paris* **310**(II):771–778.

Eissen, J. P., Nohara, M., and Cotten, J. 1994. North Fiji Basin basalts and their magma sources. 1: Incompatible element constraints, *Mar. Geol.* **116**:163–178.

Falvey, D. A. 1975. Arc reversals, and a tectonic model for the North Fiji Basin, *Austr. Soc. Explor. Geophys. Bull.* **6**:47–49.

Falvey, D. A. 1978. Analysis of paleomagnetic data from the New Hebrides, *Austr. Soc. Explor. Geophys. Bull.* **9**(3):117–123.

Francheteau, J., Yelles-Chaouche, A., and Craig, H. 1987. The Juan Fernandez microplate north of the Nazca–Pacific–Antarctic plate junction at 35°S, *Earth Planet. Sci. Lett.* **86**:253–286.

Gente, P., Mével, C., Auzende, J. M., Karson, J. A., and Fouquet, Y. 1991. An example of recent accretion on the Mid-Atlantic Ridge: The Snake Pit neovolcanic ridge (MARK area, 23°22'N), *Tectonophysics* **190**:1–29.

Gill, J. B. 1981. *Orogenic Andesites and Plate Tectonics*, Springer-Verlag, Berlin.

Gill, J. B. 1984. Sr-Pb-Nd isotopic evidence that both MORB and OIB sources contribute to oceanic island arc magmas in Fiji, *Earth Planet. Sci. Lett.* **68**:443–458.

Gill, J. B., and Gorton M. 1973. A proposed geological and geochemical history of eastern Melanesia, in *The Western Pacific: Island Arcs, Marginal Seas and Geochemistry* (P. J. Coleman, ed.), pp. 543–566, University of Western Australia Press.

Gracia-Mont, E. 1991. Etude morphostructurale du segment N160° la dorsale du Basin Nord-Fidjien, Analyse des données de la campagne Yokosuka 90, Rapport de D.E.A., Université de Bretagne Occidentale, Brest.

Gracia-Mont, E. 1992. El segment N160 de la Conca Nord-Fijiana (Pacific Sud-Oest): Morfoestructura d'un eix d'acrecio oceanica d'edat quaternaria dins una conca marginal, Tesi de Licenciatura, Universitat de Barcelona, Barcelona.

Gracia-Mont, E., Ondréas, H., Bendel, V., and STARMER Group. 1994. Multiscale morphologic variability of the North Fiji Basin Ridge (Southwest Pacific), *Mar. Geol.* **116**:133–162.

Grimaud, D., Ishibashi, J. I., Lagabrielle, Y., Auzende, J. M., and Urabe, T. 1991. Chemistry of hydrothermal fluids from the 17°S active site on the North Fiji Basin Ridge (SW Pacific), *Chem. Geol.* **93**:209–218.

Gutenberg, B., and Richter C. F. 1954. *Seismicity of the Earth*, 2nd ed., Princeton University Press, Princeton, NJ.

Halunen, A. J., Jr. 1979. Tectonic history of the Fiji Plateau, Ph.D. thesis, University of Hawaii, Honolulu.

Hey, R. N., Kleinrock, M. C., Miller, S. P., Atwater, T. M., and Searle, R. C. 1986. Sea Beam/Deep-Tow investigation of an active oceanic propagating rift system, Galapagos 95.5°W, *J. Geophys. Res.* **91**:3369–3393.

Hamburger, M. W., and Isacks, B. L. 1988. Diffuse backarc deformation in the Southwestern Pacific, *Nature* **332**:599–604.

Hamburger, M. W., and Isacks, B. L. 1994. Shallow seismicity in the North Fiji Basin, in *Basin Formation, Ridge Crest Processes, and Metallogenesis in the North Fiji Basin* (L. W. Kroenke and J. V. Eade, eds.), pp. 21–32, Circum-Pacific Council for Energy and Mineral Resources. Earth Science Series, Vol. 15.

Hawkins, J. W., and Melchior J. T. 1985. Petrology of Mariana Trough and Lau Basin basalts, *J. Geophys. Res.* **90**:11,431–11,468.

Huchon, P., Gracia, E., Ruellan, E., Joshima, M., and Auzende, J. M. 1994. Kinematics of active spreading in the central North Fiji Basin (Southwest Pacific), *Mar. Geol.* **116**:69–88.

Hughes Clarke, J. E., Jarvis, P., Tiffin, D., Price, R., and Kroenke, L. 1993. Tectonic activity and plate boundaries along the northern flank of the Fiji Platform, *Geo-Mar. Lett.* **13**:98–106.

Ishibashi, J.-I., Grimaud, D., Nojiri, Y., Auzende, J. M., and Urabe, T. 1994. Fluctuation of chemical compositions of the phase-separated hydrothermal fluid from the North Fiji Basin Ridge, *Mar. Geol.* **116**:215–226.

James, A., and Falvey, D. A. 1978. Analysis of paleomagnetic data from Viti Levu, Fiji, *Austr. Soc. Explor. Geophys. Bull.* **9**:15–123.

Jarvis, P., Hughes-Clarke, J., Tanahashi, M., Tiffin, D., and Kroenke, L. 1994. The western Fiji Transform Fault and its role in the dismemberment of the Fiji Platform, *Mar. Geol.* **116**:57–68.

Jarvis, P., Kroenke, L., Price, R., and Maillet, P. 1993. GLORIA imagery of sea floor structures in the northern North Fiji Basin, *Geo-Mar. Lett.* **13**:90–97.

Johnson, D. P., Maillet, P., and Price, P. 1993. Regional setting of a complex backarc: New Hebrides arc, northern Vanuatu-eastern Solomon Islands, *Geo-Mar. Lett.* **13**:82–89.

Johnson, K. T. M., and Sinton, J. M. 1990. Petrology, tectonic setting and the formation of backarc basin basalts in the North Fiji Basin, *Geol. Jb. D* **92**:517–545.

Kappel, E. S., and Ryan, W. B. F. 1986. Volcanic episodicity and a non-steady state rift valley along Northeast Pacific spreading centers: Evidence from SeaMarc I, *J. Geophys. Res.* **91**(13):13,925–13,940.

Karson, J. A. 1990. Seafloor spreading of the Mid-Atlantic Ridge: Implications for the structure of ophiolites and oceanic lithosphere produced in slow-spreading environments, in *Proceedings of the Symposium "Troodos 1987"* (J. Malpas, E. M. Moores, A. Panayiotou, and C. Xanophontos, eds.), Geological Survey Department, Nicosia, Cyprus.

Karson, J. A., Thompson, G., Humphries, S. E., Edmond, J. M., Bryan, W. B., Brown, J. R., Winters, A. T., Pockalny, R. A., Casey, J. F., Campbell, A. C., Klinkhammer, G., Palmer, M. R., Kinzler, R. J., and Sulanovska, M. M. 1987. Along axis variations in seafloor spreading in the MARK area, *Nature* **328**: 681–685.

Kleinrock, M. C. in press. The southern boundary of the Juan Fernandez microplate: braking microplate rotation and deformation of the Antarctic plate, *J. Geophys. Res.*

Kroenke, L. W., Eade, J. V., Yan, C. Y., and Smith, R. 1994. Sediment distribution in the north-central North Fiji Basin, in *Basin Formation, Ridge Crest Processes, and Metallogenesis in the North Fiji Basin* (L. W. Kroenke and J. V. Eade, eds.), pp. 63–73, Circum-Pacific Council Energy and Mineral Resources, Springer, Heidelberg. Earth Science Series, Vol. 153.

Kroenke, L. W., Jarvis, P., and Price, R. C. 1987, Morphology of the Fiji Fracture Zone: Recent reorientation of plate boundaries in the vicinity of the North Fiji Basin, *Eos* **68**(44):1445.

Kroenke, L. W., Price R. C., and Jarvis P. A. 1991. North Fiji Basin, 1:250,000, Pacific Seafloor Atlas, Hawaii Institute of Geophysics, Honolulu, HI, sheets 10 to 17.

Lafoy, Y., Auzende, J. M., Gente, P., and Eissen, J. P. 1987. L'extremité occidentale de la zone de fracture Fidjienne et le point triple de 16°40S, Résultats du Leg III de la campagne SEAPSO du N.O. Jean Charcot (Décembre 1985) dans le bassin Nord Fidjien, SW Pacifique, *C.R. Acad. Sci. Paris* **304**:147–152.

Lafoy, Y., Auzende, J. M., Ruellan, E., Huchon, P., and Honza, E. 1990. The 16°40S triple junction in the North Fiji Basin (SW Pacific), *Mar. Geophys. Res.* **12**:285–296.

Lagabrielle, Y., Auzende, J. M., Eissen, J. P., Janin, M. C., and Cotten, J. 1994. Geology and geochemistry of a 800 m section through young upper oceanic crust in the North Fiji Basin (Southwest Pacific), *Mar. Geol.* **116**: 113–132.

Larson, R. L., Searle, R. C., Kleinrock, M. C., Shouten, H., Bird, R. T., Naar, D. F., Rusby, R. I., Hooft, E. E., and Lasthiotakis, H. 1992. Roller-bearing tectonic evolution of the Juan Fernandez microplate, *Nature* **356**: 571–576.

Larue, B. M., Pontoise, B., Malahoff, A., Lapouille, A., and Latham, G. V. 1982. Bassins marginaux actifs du Sud-Ouest Pacifique: Plateau Nord-Fidjien, bassin de Lau, in *Contribution à l'étude géodynamique du Sud-Ouest Pacifique*, Equipe de Géologie-Géophysique du Centre ORSTOM de Nouméa. Travaux et Documents de l'ORSTOM **147**:363–406.

Louat, R. 1982. Séismicité et subduction de la terminaison sud de l'arc insulaire des Nouvelles Hébrides, in *Contribution à l'étude géodynamique du Sud-Ouest Pacifique*, Equipe de Géologie-Géophysique du Centre ORSTOM de Nouméa. Travaux et Documents de l'ORSTOM **147**:179–185.

Louat, R., and Pelletier, B. 1989. Seismotectonic and present-day relative plate motions in the New Hebrides–North Fiji Basin region, *Tectonophysics* **167**:41–55.

Luyendyck, B. P., Bryan, W. B., and Jezek, P. A. 1974. Shallow structure of the New Hebrides island arc, *Geol. Soc. Am. Bull.* **85**:1287–1300.

Macdonald, K. C. 1983. Crustal processes at spreading centers, *Rev. Geophys.* **21**:1441–1453.

Macdonald, K. C., Luyendyck, B. P., and Von Herzen, R. P. 1973. Heat flow and plate boundaries in Melanesia, *J. Geophys. Res.* **78**:2537–2546.

Macdonald, K. C., Sempère, J. C., and Fox, P. J. 1984. The East Pacific Rise from the Siqueiros of the Orozco fracture zone: Along strike continuity of the neovolcanic zone and the structure and evolution of overlapping spreading centers, *J. Geophys. Res.* **89**:6049–6069.

Maillet, P., Eissen, J. P., Lapouille, A., Monzier, M., Baleivanualala, V., Butscher, J., Gallois, F., and Lardy, M.

1986. La dorsale active du bassin Nord-Fidjien entre 20°S et 20°53′S: Signature magnétique et morphologique, *C.R. Acad. Sci. Paris* **302**(II):135–140.
Maillet, P., Monzier M., Eissen, J. P., and Louat R. 1989. Geodynamics of an arc ridge junction: The case of the New Hebrides arc–North Fiji Basin, *Tectonophysics* **165**:251–268.
Malahoff, A., Feden, R. H., and Fleming, H. F. 1982a. Magnetic anomalies and tectonic fabric of marginal basins north of New Zealand, *J. Geophys. Res.* **87**:4109–4125.
Malahoff, A., Hammond, S. R., Naughton, J. J., Keeling, D. L., and Richmond, R. N. 1982b. Geophysical evidence for post-Miocene rotation of the island of Viti Levu, Fiji, and its relationship to the tectonic development of the North Fiji Basin, *Earth Planet. Sci. Lett.* **57**:398–414.
Malahoff, A., Kroenke, L. W., Cherkis, N., and Brozena, J. 1994. Magnetic and tectonic fabric of the North Fiji Basin and Lau Basin, in *Basin Formation, Ridge Crest Processes, and Metallogenesis in the North Fiji Basin* (L. W. Kroenke and J. V. Eade, eds.), Earth Science Ser., Vol. 15, pp. 49–61, Circum-Pacific Council for Energy and Mineral Resources.
Mammerickx, J., Chase, T. E., Smith, S. M., and Taylor, I. L. 1971. Bathymetry of the South Pacific, chart n°12. Scripps Institution of Oceanography.
Massoth, G. J., Butterfield, D. A., Lupton, J. E., McDuff, R. E., Lilley, M. D., and Jonasson, I. R. 1989. Submarine venting of phase-separated hydrothermal fluids at axial volcano, Juan de Fuca Ridge, *Nature* **340**:702–705.
Monjaret, M. C., Bellon, H., and Maillet, P. 1991. Magmatism of the troughs behind the New Hebrides island arc (R.V. *Jean Charcot* SEAPSO 2 cruise): K-Ar geochronology and petrology, *J. Volcanol. Geotherm. Res.* **46**:265–280.
Monzier, M., Collot, J. Y., and Daniel, J. 1984. Carte bathymétrique des parties centrale et méridionale de l'arc insulaire des Nouvelles-Hébrides. Office de la Recherche Scientifique et Technique Outre-Mer, Editions de l'ORSTOM, Paris.
Monzier, M., Daniel, J., and Maillet, P. 1990. La collision ride des Loyauté/arc des Nouvelles-Hébrides (Pacifique Sud-Ouest), *Oceanol. Acta* **10**:43–56.
Monzier, M., Maillet, P., and Dupont, J. 1991. Carte bathymétrique des parties méridionales de l'arc insulaire des Nouvelles-Hébrides et du bassin Nord-Fidjien, Institut Français de Recherche Scientifique pour le Développement en Coopération, Editions de l'ORSTOM, Paris.
Nohara, M., Hirose, K., Eissen, J. P., Urabe, T., and Joshima, M. 1994. North Fiji Basin basalts and their magma sources. II: Sr-Nd isotopic and trace element constraints, *Mar. Geol.* **116**:179–196.
Nojiri, Y., Ishibashi, J. I., Kawai, T., Otsuki, A., and Sakai, H. 1989. Hydrothermal plumes along the North Fiji Basin spreading axis, *Nature* **342**:667–670.
Ondréas, H., Ruellan, E., Auzende, J. M., Bendel, V., de Alteriis, G., Gracia-Mont, E., Lagabrielle, Y., and Tanahashi, M. 1993. Variabilité morpho-structurale à l'échelle kilométrique de la dorsale du Bassin Nord Fidjien: Exploration in situ du segment compris enter 18°50′S et 19°S, *C.R. Acad. Sci. Paris* **316**(II):115–122.
Pelletier, B., Charvis, P., Daniel, J., Hello, Y., Jamet, F., Louat, R., Nanau, P., and Rigolot, P. 1988. Structure et linéations magnétiques dans le coin nord-ouest du bassin Nord-Fidjien: Résultats préliminaires de la campagne EVA 14 (août 1987), *C.R. Acad. Sci. Paris,* **306**(II):1247–1254.
Pelletier, B., Lafoy, Y., and Missegue, F. 1993a. Morphostructure and magnetic fabric of the northwestern North Fiji Basin, *Geophys. Res. Lett.* **20**(12):1151–1154.
Pelletier, B., and Louat, R. 1989. Mouvement relatif des plaques dans le Sud-Ouest Pacifique, *C.R. Acad. Sci. Paris* **308**:123–130.
Pelletier, B., Missègue, F., Lafoy, Y., Mollard, L., Decourt, R., Dupont, J., Join, Y., Perrier, J., and Récy, J. 1993b. Extrémités nord du bassin Nord-Fidjien et des fossés arrière-arc des Nouvelles-Hébrides: Morphostructure et signature magnétique, *C.R. Acad. Sci. Paris* **316**(II):637–644.
Price, R. C., Johnson, L. E., and Crawford, A. J. 1990. Basalts of the North Fiji basin: The generation of back arc basin magmas by mixing of depleted and enriched mantle sources, *Contrib. Mineral. Petrol.* **105**:106–121.
Price, R. C., and Kroenke, L. W. 1991. Tectonics and magma genesis in the northern North Fiji Basin, *Mar. Geol.* **98**:241–258.
Price, R. C., Maillet, P., and Johnson, D. A. 1993. Interpretation of GLORIA side-scan sonar imagery for the Coriolis Troughs of the New Hebrides backarc, *Geo-Mar. Lett.* **13**:71–81.
Price, R. C., Maillet, P., McDougall, I., and Dupont, J. 1991. The geochemistry of basalts from the Wallis Islands, Northern Melanesian Borderland: Evidence for a lithospheric origin for Samoan-type basaltic magmas, *J. Volcanol. Geotherm. Res.* **45**:267–288.
Récy, J., Pelletier, B., Charvis, P., Gerard, M., Monjaret, MC., and Maillet, P. 1990. Structure, âge et origine des fossés arrière-arc des Nouvelles-Hébrides (Sud-Ouest Pacifique) *Oceanol. Acta* **10**:165–182.

Ruellan, E., Auzende, J. M., Honza, E., and the STARMER Group. 1989. L'accrétion dans le bassin Nord Fidjien méridional: Premiers résultats de la campagne franco-japonaise STARMER/KAIYO 88, *C.R. Acad. Sci. Paris* **309**(II):1247–1254.

Ruellan, E., Huchon P., Auzende, J. M., and Gracia, E. 1994. Propagating rift and overlapping spreading center in the North Fiji Basin, *Mar. Geol.* **116**:37–56.

Saunders, A. D., and Tarney, J. 1984. Geochemical characteristics of basaltic volcanism within backarc basins, in *Marginal Basins: Geology, Volcanism and Associated Sedimentary and Tectonic Processes in Modern and Ancient Marginal Basins* (B. P. Kokelaar and M. F. Holwells, eds.), pp. 59–76, Blackwell, Oxford.

Sclater, J. G., and Francheteau, J. 1970. The implications of terrestrial heat flow observations on current tectonic and geochemical models of the crust and upper mantle of the earth, *Geophys. J. R. Astron. Soc.* **20**:509–542.

Sclater, J. G., and Menard, H. W. 1967. Topography and heat flow of the Fiji Plateau, *Nature* **216**:991–993.

Sinton, J. M., and Fryer, P. 1987. Mariana lavas from 18°N: Implications for the origin of back arc basin basalts, *J. Geophys. Res.* **92**(B12):782–802.

Sinton, J. M., Johnson K. T. M., and Price R. C. 1985. Petrology and geochemistry of volcanic rocks from the Northern Melanesian Borderland, in *Investigations of the Northern Melanesian Borderland* (T. M. Brocher, ed.), Earth Science Ser., Vol. 3, pp. 35–65, Circum-Pacific Council for Energy and Mineral Resources, Houston, TX.

Sinton J. M., Price, R. C., Johnson, K. T. M., Staudigel, H., and Zindler, A. 1994. Petrology and geochemistry of submarine lavas from the Lau and North Fiji Back-Arc Basins, in *Basin Formation, Ridge Crest Processes, and Metallogenesis in the North Fiji Basin* (L. W. Kroenke and J. V. Eade, eds.), Earth Science Ser., Vol. 15, pp. 119–135, Circum-Pacific Council for Energy and Mineral Resources.

Stackelberg, U. von, and Rad, U. von. 1990. Geological evolution and hydrothermal activity in the Lau and North Fiji basins (Sonne Cruise SO-35)—a synthesis, *Geol. Jb.* **92**:629–660.

Stackelberg, U. von, and Shipboard Scientific Party. 1985. Hydrothermal sufide deposits in backarc spreading centers in the Southwest Pacific, BGR Bundesandstalt für Geowissenschaften und Röstoffe Circular **2**:3–14.

Sun, S. S., and McDonough, W. F. 1989. Chemical and isotopic systematics of oceanic basalts: Implications for mantle composition and processes, in *Magmatism in the Ocean Basins* (A. D. Saunders and M. J. Norry, eds.), Geol. Soc. Spec. Publ. **42**:313–345.

Sykes, L. R. 1966. The seismicity and deep structure of islands arcs, *J. Geophys. Res.* **71**:2981–3006.

Sykes, L. R., Isacks, B. L., and Oliver, J. 1969. Spatial distribution of deep and shallow earthquakes of small magnitudes in the Fiji–Tonga region, *Bull. Seismol. Soc. Am.* **59**:1093–1113.

Urabe, T., Auzende, J. M., *et al.* 1992. Bathymetric map of the central part of the North Fiji Basin, Southwest Pacific, between 14°20S and 21°50S, 2 colored maps, scale: 1/500 000, Published under the Special Coordination for Promoting Science and Technology (Japan).

Von Damm, K. L., and Bischoff, J. L. 1987. Chemistry of hydrothermal solutions from the Juan de Fuca Ridge, *J. Geophys. Res.* **92**:11,334–11,346.

Wright, E., and White, W. M. 1987. The origin of Samoa: New evidence from Sr, Nd, and Pb isotopes, *Earth Planet. Sci. Lett.* **81**:151–162.